J. Fluid Mech. (2014), *vol.* 757, *pp.* 114–154.
doi:10.1017/jfm.2014.490

Weak turbulence theory for rotating magnetohydrodynamics and planetary flows

Sébastien Galtier[1,†]

[1]Laboratoire de Physique des Plasmas, École Polytechnique, F-91128 Palaiseau CEDEX, France

(Received 27 March 2014; revised 11 July 2014; accepted 21 August 2014; first published online 19 September 2014)

A weak turbulence theory is derived for magnetohydrodynamics (MHD) under rapid rotation and in the presence of a uniform large-scale magnetic field which is associated with a constant Alfvén velocity $\boldsymbol{b}_0$. The angular velocity $\boldsymbol{\Omega}_0$ is assumed to be uniform and parallel to $\boldsymbol{b}_0$. Such a system exhibits left and right circularly polarized waves which can be obtained by introducing the magneto-inertial length $d \equiv b_0/\Omega_0$. In the large-scale limit ($kd \to 0$, with k being the wavenumber) the left- and right-handed waves tend to the inertial and magnetostrophic waves, respectively, whereas in the small-scale limit ($kd \to +\infty$) pure Alfvén waves are recovered. By using a complex helicity decomposition, the asymptotic weak turbulence equations are derived which describe the long-time behaviour of weakly dispersive interacting waves via three-wave interaction processes. It is shown that the nonlinear dynamics is mainly anisotropic, with a stronger transfer perpendicular than parallel to the rotation axis. The general theory may converge to pure weak inertial/magnetostrophic or Alfvén wave turbulence when the large- or small-scale limits are taken, respectively. Inertial wave turbulence is asymptotically dominated by the kinetic energy/helicity, whereas the magnetostrophic wave turbulence is dominated by the magnetic energy/helicity. For both regimes, families of exact solutions are found for the spectra, which do not correspond necessarily to a maximal helicity state. It is shown that the hybrid helicity exhibits a cascade whose direction may vary according to the scale k_f at which the helicity flux is injected, with an inverse cascade if $k_f d < 1$ and a direct cascade otherwise. The theory is relevant to the magnetostrophic dynamo, whose main applications are the Earth and the giant planets, such as Jupiter and Saturn, for which a small ($\sim 10^{-6}$) Rossby number is expected.

Key words: dynamo theory, MHD turbulence, wave–turbulence interactions

1. Introduction

Rotation is a commonly observed phenomenon in astronomy: planets, stars and galaxies all spin around their axis. The rotation rate of planets in the solar system was first measured by tracking visual features, whereas stellar rotation is generally measured through Doppler shift or by following the magnetic activity (Tassoul 2000). One consequence of the Sun's rotation is the formation of the Parker interplanetary magnetic field spiral (Parker 1958), which is well detected by space crafts. The Earth's

† Email address for correspondence: sebastien.galtier@lpp.polytechnique.fr

rotation has a strong impact on the turbulent dynamics of large-scale geophysical flows (Shirley & Fairbridge 1997). These examples show that the study of rotating flows is of interest in many areas, ranging from engineering (turbomachinery) to geophysics (oceans, the Earth's atmosphere, gaseous planets), weather prediction and turbulence (Davidson 2004). Rotation is often coupled with other dynamical factors; it is therefore important to isolate the effect of the Coriolis force to understand precisely its impact. The importance of rotation can be measured with the Rossby number

$$Ro = \frac{U_0}{L_0 \varOmega_0}, \tag{1.1}$$

where U_0, L_0 and $\varOmega_0$ are, respectively, the typical velocity, length scale and rotation rate. This dimensionless number measures the ratio of the advection term to the Coriolis force in the Navier–Stokes equations; a small value of Ro means that the dynamics is driven mainly by rotation. Typical large-scale planetary flows are characterized by $Ro \sim 0.1$ (Shirley & Fairbridge 1997), whereas liquid metals (mainly iron) in the Earth's outer core are much more affected by rotation, with $Ro \sim 10^{-6}$ (Roberts & King 2013). Note that for a giant planet like Jupiter in which liquid metallic hydrogen is present in most of the planet's volume, it is believed that the Rossby number may be even smaller (see e.g. Jones 2011). These situations contrast with the solar convective region where the magnetic field is believed to be magnified and for which $Ro \sim 1$.

Inertial waves are a ubiquitous feature of neutral fluids under rapid rotation (Greenspan 1968). Although much is known about their initial excitation, their nonlinear interactions are still a subject of intensive research. Many papers have been devoted to pure rotating turbulence ($Ro \leqslant 1$), but because of the different nature of the investigations (theoretical, numerical and experimental), it is in general difficult to compare directly the results obtained. From a theoretical point of view, it is convenient to use a spectral description in terms of continuous wavevectors along with the unbounded homogeneity assumption in order to derive the governing equations for the energy, kinetic helicity and polarization spectra (Cambon & Jacquin 1989). Although such equations introduce transfer terms which still need to be evaluated consistently, it is already possible to show, using a weakly nonlinear resonant waves analysis (Waleffe 1993), the anisotropic nature of that turbulence, with a nonlinear transfer preferentially in the perpendicular (to $\boldsymbol{\varOmega}_0 = \varOmega \boldsymbol{e}_\parallel$) direction. For moderate Rossby numbers the eddy-damped quasinormal Markovian model may be used as a closure (Cambon, Mansour & Godeferd 1997), whereas in the small-Rossby-number limit the asymptotic weak turbulence theory can be derived rigorously (Galtier 2003). In the latter case, it was shown that the wave modes ($k_\parallel > 0$) are decoupled from the slow mode ($k_\parallel = 0$), which is not accessible by the theory, and the positive energy flux spectra were also obtained as exact power-law solutions. The weak turbulence regime was also investigated numerically; in particular, it was shown that the energy cascade goes forward (Bellet *et al.* 2006). Recently, the problem of confinement (i.e. the study of homogeneity effects due to two infinite parallel walls perpendicular to the rotation axis) has been addressed explicitly in the inertial wave turbulence theory using discrete wavenumbers (Scott 2014): three asymptotically distinct stages in the evolution of the turbulence have been found, leading finally to a regime dominated by resonant interactions. Numerical simulations are often used to investigate homogeneous rotating turbulence (see e.g. Bardina, Ferziger & Rogallo 1985; Bartello, Metais & Lesieur 1994; Mininni & Pouquet 2010*a*). Several questions have been investigated, such as the origin of the anisotropy of the flow (i.e. the fact that the turbulent cascade is mainly transverse to the rotation axis) and the origin of the inverse cascade observed when a forcing is applied at intermediate-scale k_f. However, depending on the question addressed, the results may be affected by the discretization and by finite-box effects at too-small Rossby numbers and too-long elapsed time (Smith & Lee 2005; Bourouiba 2008). In particular, this seems to be the case for the question of the inverse cascade mediated by the decoupling of the slow mode. For example, it was found that the one-dimensional isotropic energy spectrum $E(k) \sim k^{-x}$ may follow two different power laws, with $2 \leqslant x \leqslant 2.5$ at small scales ($k > k_f$) and $x \simeq 3$ at large scales ($k < k_f$) (Smith & Waleffe 1999); but it was also shown that the scaling at large scales is strongly influenced by the value of the aspect ratio between the parallel and perpendicular (to $\boldsymbol{\Omega}_0$) resolutions, such that a small aspect ratio leads to a reduction in the number of available resonant triads and hence an alteration of the spectrum, with the restoration of a $k^{-5/3}$ spectrum for sufficiently small vertical resolutions. Several experiments have been devoted to studying rotating turbulence with different types of apparatus (Hopfinger, Gagne & Browand 1982; Jacquin *et al.* 1990; Baroud *et al.* 2002; Morize, Moisy & Rabaud 2005; van Bokhoven *et al.* 2009; Rieutord *et al.* 2012). In contrast to the theory and simulations, it is very challenging to reproduce experimentally the conditions of homogeneous turbulence (see the discussion in Scott 2014). Nevertheless, one of the main results reported is that the rotation leads to bi-dimensionalisation of an initial homogeneous isotropic turbulence, with anisotropic spectra where energy is preferentially accumulated in the perpendicular (to $\boldsymbol{\Omega}_0$) wavenumbers $k_\perp$. Energy spectra with $x \geqslant 2$ were experimentally observed (Baroud *et al.* 2002; Morize *et al.* 2005; van Bokhoven *et al.* 2009), revealing a significant discrepancy with the isotropic Kolmogorov spectrum ($x = 5/3$) for non-rotating fluids. Note that the wavenumber entering into the spectral measurements corresponds mainly to $k_\perp$. Recently, direct measurements of energy transfer have been made in the physical space by using third-order structure functions (Lamriben, Cortet & Moisy 2011), and an increase of anisotropy at small scales has been found, in agreement with some theoretical studies (Jacquin *et al.* 1990; Galtier 2003; Bellet *et al.* 2006; Galtier 2009*a*). The effect of kinetic helicity – which quantifies departures from mirror symmetry (Moffatt 1969) – on rotating fluids has been the subject of few studies. One reason is that it is difficult to measure the helicity production from experiments. Another reason is probably linked to the negligible effect of helicity on energy in non-rotating turbulence. Indeed, in this case one observes a joint constant flux cascade of energy and helicity, with a $k^{-5/3}$ spectrum for both quantities (Chen, Chen & Eyink 2003*a*; Chen *et al.* 2003*b*). Recently, however, several numerical simulations have demonstrated a surprisingly strong impact of helicity on fast rotating hydrodynamic turbulence (Teitelbaum & Mininni 2009; Mininni & Pouquet 2010*a*,*b*; Mininni, Rosenberg & Pouquet 2012), the main properties of which can be summarized as follows. When the (large-scale) forcing applied to the system injects only negligible helicity, the dynamics is mainly governed by a direct energy cascade compatible with an energy spectrum of $E(k_\perp) \sim k_\perp^{-5/2}$, which is precisely the weak turbulence prediction (Galtier 2003). However, when the helicity injection becomes so important that the dynamics is mainly governed by a direct helicity cascade, different scalings are found following the empirical law

$$n + \tilde{n} = -4, \tag{1.2}$$

where n and $\tilde{n}$ are the power-law indices of the one-dimensional energy and helicity spectra, respectively. This law cannot be explained by a consistent phenomenology

https://doi.org/10.1017/jfm.2014.490 Published online by Cambridge University Press

where anisotropy is used, which renders the relation (1.2) highly non-trivial. As shown by Galtier (2014), an explanation can only be found when a rigorous analysis is conducted on the weak turbulence equations: the relation corresponds in fact to the finite helicity flux spectra, which are exact solutions of the equations.

It has been long recognized that the Earth's magnetic field is not steady (Finlay *et al.* 2010). Changes occur across a wide range of time scales, from seconds – because of interactions between the solar wind and the magnetosphere – to several tens of millions of years, which is the longest timespan between polarity reversals. To understand the generation and maintenance of a large-scale magnetic field, the most promising mechanism is the dynamo (Pouquet, Frisch & Leorat 1976; Moffatt 1978; Brandenburg 2001). The dynamo is an active area of research which has seen dramatic developments in the past few years (Dormy, Valet & Courtillot 2000). The focus of this research is primarily on the Earth, for which a large amount of data is available, allowing us to follow, for instance, occurrences of geomagnetic polarity reversal over millions of years (Finlay & Jackson 2003; Roberts & King 2013). Such chaotic behaviour contrasts drastically with the surprisingly regular behaviour of the Sun, which changes the polarity of its magnetic field lines approximately every 11 years. It is believed that the three main ingredients of the geodynamo problem are the Coriolis, Lorentz–Laplace and buoyancy forces (Finlay *et al.* 2010). This last force may be viewed as a source of turbulence for the conducting fluids described by incompressible magnetohydrodynamics (MHD), whereas the first two forces are more or less balanced. This balance leads to the strong-field regime – the so-called magnetostrophic dynamo – for which we may derive magnetostrophic waves (Lehnert 1954; Schmitt *et al.* 2008). This regime is thought to be relevant not only to the Earth but also to giant planets such as Jupiter and Saturn, and by extension probably to exoplanets as well (Stevenson 2003). In order to investigate the dynamo problem, several experiments have been developed (Pétrélis, Mordant & Fauve 2007). In one of them, the authors were able to successfully reproduce with liquid sodium reversals and excursions of a turbulent dynamo generated by two (counter-)rotating disks (Berhanu *et al.* 2007). This result follows a three-dimensional numerical simulation of the Earth's outer core, from which the reversal of the dipole moment was also obtained (Glatzmaier & Roberts 1995). In this model, however, the inertial/advection terms are simply discarded to mimic a very small Rossby number. This assumption is in apparent contradiction to any turbulent regime (the Reynolds number is approximately 10^9 for the Earth's outer core; see Finlay *et al.* 2010) and in particular to the weak turbulence regime in which the nonlinear interactions – though weak at short time scales compared with the linear contributions – become important for the nonlinear dynamics at asymptotically large time scales. As we will see below, this is basically the regime that we investigate theoretically in this paper; a sea of helical (magnetized) waves (Moffatt 1970) will be considered as the main ingredient for the triggering of the dynamo through nonlinear transfer of the magnetic energy and helicity. (In weak turbulence the main ingredients are waves instead of eddies: it is the cumulative weak interactions of many dispersive waves that produces a weak turbulence cascade; also, we shall often talk about a sea of waves to characterize this regime.)

Weak turbulence is the study of the long-time statistical behaviour of a sea of weakly nonlinear dispersive waves (Nazarenko 2011). The energy transfer between waves occurs mostly among resonant sets of waves, and the resulting energy distribution, far from thermodynamic equilibrium (a source is supposed to be present to feed the turbulence and prevent the flow from reaching a state where the energy flux through scales is null; see Zakharov, L'Vov & Falkovich 1992), is characterized by a wide power-law spectrum and a high Reynolds number. This range of wavenumbers – the inertial range – is generally localized between large scales, at which energy is injected into the system (sources), and small scales, at which waves break or dissipate (sinks). Pioneering works on weak turbulence date back to the 1960s, when it was established that the stochastic initial value problem for weakly coupled wave systems has a natural asymptotic closure induced by the dispersive nature of the waves and the large separation of linear and nonlinear time scales (Benney & Saffman 1966; Benney & Newell 1967, 1969). In the meantime, Zakharov & Filonenko (1966) showed that the kinetic equations derived from the weak turbulence analysis have exact equilibrium solutions which are the thermodynamic zero-flux solutions and are also – more importantly – finite-flux solutions that describe the transfer of conserved quantities between sources and sinks. The solutions, first published for isotropic turbulence (Zakharov 1965; Zakharov & Filonenko 1966) were then extended to anisotropic turbulence (Kuznetsov 1972). Weak turbulence is a very common natural regime with applications, for example, to capillary waves (Kolmakov *et al.* 2004), gravity waves (Falcon, Laroche & Fauve 2007), superfluid helium and processes of Bose–Einstein condensation (Lvov, Nazarenko & West 2003), nonlinear optics (Dyachenko *et al.* 1992), inertial waves (Galtier 2003), Alfvén waves (Galtier *et al.* 2000, 2002; Galtier & Chandran 2006) and whistler/kinetic Alfvén waves (Galtier 2006*b*).

In this paper, the weak turbulence theory will be established for rotating MHD in the limit of small Rossby and Ekman numbers, where the latter measures the ratio of the viscous to Coriolis terms. We shall assume the existence of a strong uniform magnetic field parallel to the fast and constant rotation rate. The combination of the Coriolis and Lorentz–Laplace forces leads to the appearance of two types of circularly polarized waves and a possible non-equipartition between the kinetic and magnetic energies (Moffatt 1972; Favier, Godeferd & Cambon 2012). After a general introduction to rotating MHD in § 2, a weak helical turbulence formalism is developed in § 3 by using a technique from Galtier (2006*b*). The phenomenology of the weak turbulence dynamo is given in § 4, the general properties of the weak turbulence equations are discussed in § 5, and the exact spectral solutions are derived in § 6. We conclude with a discussion in § 7.

2. Rotating magnetohydrodynamics

2.1. *Governing equations*

The basic equations governing incompressible MHD under solid rotation and in the presence of a uniform background magnetic field are

$$\frac{\partial \boldsymbol{u}}{\partial t} + 2\boldsymbol{\Omega}_0 \times \boldsymbol{u} + \boldsymbol{u} \cdot \nabla\, \boldsymbol{u} = -\nabla P_* + \boldsymbol{b}_0 \cdot \nabla\, \boldsymbol{b} + \boldsymbol{b} \cdot \nabla\, \boldsymbol{b} + \nu \nabla^2 \boldsymbol{u}, \tag{2.1}$$

$$\frac{\partial \boldsymbol{b}}{\partial t} + \boldsymbol{u} \cdot \nabla\, \boldsymbol{b} = \boldsymbol{b}_0 \cdot \nabla\, \boldsymbol{u} + \boldsymbol{b} \cdot \nabla\, \boldsymbol{u} + \eta \nabla^2 \boldsymbol{b}, \tag{2.2}$$

$$\nabla \cdot \boldsymbol{u} = 0, \tag{2.3}$$

$$\nabla \cdot \boldsymbol{b} = 0, \tag{2.4}$$

where $\boldsymbol{u}$ is the velocity, P_* is the total pressure (including the magnetic pressure and the centrifugal term), $\boldsymbol{b}$ is the magnetic field normalized with respect to a velocity ($\boldsymbol{b} \to \sqrt{\mu_0 \rho_0}\, \boldsymbol{b}$, with ρ_0 the constant density), $\boldsymbol{b}_0$ is the uniform normalized magnetic field, Ω_0 is the rotation rate, ν is the kinematic viscosity and η is the magnetic diffusivity. The Coriolis force appears in the first equation (second term in the left-hand side). Note that the magnetic field $\boldsymbol{b}_0$ must be interpreted in the context of planetary dynamos as an external dipolar field. Turbulence can be maintained only if a source is added to balance the small-scale dissipation. For example, in the geodynamo problem, we may think of the role of external forcing as being played by the convection (since the Rayleigh number is approximately 10^9) along with the buoyancy force (Braginsky & Roberts 1995). In our case, we shall perform a purely nonlinear analysis, so the source and dissipation terms will be discarded. The weak turbulence equations that will be derived can describe, however, different magnetic Prandtl limits since the (linear) dissipative terms can be added to the equations after the nonlinear asymptotic analysis is performed (see the end of appendix C). In the rest of the paper, we shall assume that

$$\boldsymbol{\Omega}_0 = \Omega_0 \hat{\boldsymbol{e}}_\parallel, \quad \boldsymbol{b}_0 = b_0 \hat{\boldsymbol{e}}_\parallel, \tag{2.5a,b}$$

with $\hat{\boldsymbol{e}}_\parallel$ a unit vector ($|\hat{\boldsymbol{e}}_\parallel| = 1$). We introduce the magneto-inertial length d, defined as

$$d \equiv \frac{b_0}{\Omega_0}. \tag{2.6}$$

This length scale will be useful for characterizing the main properties of rotating MHD. A physical meaning of d can be obtained by taking the ratio between the Lorentz–Laplace force and the Coriolis force, which gives, dimensionally,

$$\mathscr{M} = \frac{|\boldsymbol{b}_0 \cdot \nabla \boldsymbol{b}|}{|2\boldsymbol{\Omega}_0 \times \boldsymbol{u}|} \sim \frac{b}{u}\frac{d}{\ell} \tag{2.7}$$

with $\nabla \sim 1/\ell$. We see that d gives a scale of reference for measuring the dimensionless number $\mathscr{M}$ when b/u is known (and vice versa); thus, it is not the value of d that is important but the ratio d/ℓ. For example, when $d/\ell \gg 1$ (MHD limit) an equipartition between the fluctuating kinetic and magnetic energies is expected ($u \sim b$), which corresponds to $\mathscr{M} \gg 1$, whereas when $d/\ell \ll 1$ a balance between the Lorentz–Laplace and Coriolis forces ($\mathscr{M} \sim 1$) is expected, which means that $b \gg u$.

2.2. *Three-dimensional inviscid invariants*

The two inviscid ($\nu = \eta = 0$) quadratic invariants of incompressible rotating MHD in the presence of a background magnetic field parallel to the rotation axis are the total energy,

$$E = \frac{1}{2}\int (\boldsymbol{u}^2 + \boldsymbol{b}^2)\,\mathrm{d}\mathscr{V}, \tag{2.8}$$

and the hybrid helicity,

$$H = \frac{1}{2}\int \left(\boldsymbol{u}\cdot\boldsymbol{b} - \frac{\boldsymbol{a}\cdot\boldsymbol{b}}{d}\right)\mathrm{d}\mathscr{V}, \tag{2.9}$$

where $\boldsymbol{a}$ is the vector potential ($\boldsymbol{b} = \nabla \times \boldsymbol{a}$) and $\mathscr{V}$ is the volume over which the average is taken. The second invariant is a mixture of cross-helicity, $H^c = (1/2)\int(\boldsymbol{u}\cdot\boldsymbol{b})\,\mathrm{d}\mathscr{V}$, and magnetic helicity, $H^m = (1/2)\int(\boldsymbol{a}\cdot\boldsymbol{b})\,\mathrm{d}\mathscr{V}$, which are not conserved in the present situation (Matthaeus & Goldstein 1982). Indeed, it is straightforward to show from (2.1)–(2.4) that (see also Shebalin 2006)

$$\frac{\partial E}{\partial t} = -\int (\nu \boldsymbol{w}^2 + \eta \boldsymbol{j}^2)\, \mathrm{d}\mathscr{V}, \tag{2.10}$$

$$\frac{\partial H^c}{\partial t} = \boldsymbol{\Omega}_0 \cdot \int (\boldsymbol{b} \times \boldsymbol{u})\, \mathrm{d}\mathscr{V} - (\nu + \eta) \int (\boldsymbol{j} \boldsymbol{\cdot} \boldsymbol{w})\, \mathrm{d}\mathscr{V}, \tag{2.11}$$

$$\frac{\partial H^m}{\partial t} = \boldsymbol{b}_0 \cdot \int (\boldsymbol{b} \times \boldsymbol{u})\, \mathrm{d}\mathscr{V} - 2\eta \int (\boldsymbol{j} \boldsymbol{\cdot} \boldsymbol{b})\, \mathrm{d}\mathscr{V}, \tag{2.12}$$

where $\boldsymbol{w}$ is the vorticity and $\boldsymbol{j}$ the normalized current density. Therefore, the above equations demonstrate that a second invariant may emerge if and only if $\boldsymbol{b}_0 = d\boldsymbol{\Omega}_0$. Below, we will verify that for the weak turbulence equations these two inviscid invariants are conserved for each triad of wavevectors.

2.3. *Helical MHD waves*

One of the main effects induced by the Coriolis force is modification of the polarization of the linearly polarized Alfvén waves (solutions of the standard MHD equations), which become circularly polarized and dispersive (Lehnert 1954). Indeed, if we linearize (2.1)–(2.4) such that

$$\boldsymbol{b}(\boldsymbol{x}) = \epsilon\, \boldsymbol{b}(\boldsymbol{x}), \quad \boldsymbol{u}(\boldsymbol{x}) = \epsilon\, \boldsymbol{u}(\boldsymbol{x}), \tag{2.13a,b}$$

with ϵ being a small parameter ($0 < \epsilon \ll 1$) and $\boldsymbol{x}$ a three-dimensional displacement vector, then we obtain the following inviscid ($\nu = 0$) and ideal ($\eta = 0$) equations in Fourier space:

$$\partial_t \boldsymbol{w}_{\boldsymbol{k}} - 2\mathrm{i}k_\parallel \Omega_0 \boldsymbol{u}_{\boldsymbol{k}} - \mathrm{i}k_\parallel b_0 \boldsymbol{j}_{\boldsymbol{k}} = \epsilon\, \{\boldsymbol{w} \boldsymbol{\cdot} \nabla\, \boldsymbol{u} - \boldsymbol{u} \boldsymbol{\cdot} \nabla\, \boldsymbol{w} + \boldsymbol{b} \boldsymbol{\cdot} \nabla \boldsymbol{j} - \boldsymbol{j} \boldsymbol{\cdot} \nabla\, \boldsymbol{b}\}_{\boldsymbol{k}}, \tag{2.14}$$

$$\partial_t \boldsymbol{b}_{\boldsymbol{k}} - \mathrm{i}k_\parallel b_0 \boldsymbol{u}_{\boldsymbol{k}} = \epsilon\, \{\boldsymbol{b} \boldsymbol{\cdot} \nabla\, \boldsymbol{u} - \boldsymbol{u} \boldsymbol{\cdot} \nabla\, \boldsymbol{b}\}_{\boldsymbol{k}}, \tag{2.15}$$

$$\boldsymbol{k} \boldsymbol{\cdot} \boldsymbol{u}_{\boldsymbol{k}} = 0, \tag{2.16}$$

$$\boldsymbol{k} \boldsymbol{\cdot} \boldsymbol{b}_{\boldsymbol{k}} = 0, \tag{2.17}$$

where the wavevector $\boldsymbol{k}$ is decomposed as $\boldsymbol{k} = k\hat{\boldsymbol{e}}_k = \boldsymbol{k}_\perp + k_\parallel \hat{\boldsymbol{e}}_\parallel$ (with $k = |\boldsymbol{k}|$, $k_\perp = |\boldsymbol{k}_\perp|$ and $|\hat{\boldsymbol{e}}_k| = 1$) and $\mathrm{i}^2 = -1$. The index $\boldsymbol{k}$ denotes the Fourier transform, defined by the relation

$$\boldsymbol{u}(\boldsymbol{x}) \equiv \int \boldsymbol{u}(\boldsymbol{k})\, \mathrm{e}^{\mathrm{i}\boldsymbol{k}\cdot\boldsymbol{x}}\, \mathrm{d}\boldsymbol{k}, \tag{2.18}$$

where $\boldsymbol{u}(\boldsymbol{k}) = \boldsymbol{u}_{\boldsymbol{k}} = \tilde{\boldsymbol{u}}_{\boldsymbol{k}} \mathrm{e}^{-\mathrm{i}\omega t}$ (with the same notation as used for the other fields). The linear dispersion relation ($\epsilon = 0$) reads

$$\omega^2 + \left(\frac{2\Omega_0\, k_\parallel}{\Lambda k} \right)\, \omega - k_\parallel^2 b_0^2 = 0, \tag{2.19}$$

with

$$\begin{Bmatrix} \tilde{\boldsymbol{u}}_{\boldsymbol{k}} \\ \tilde{\boldsymbol{b}}_{\boldsymbol{k}} \end{Bmatrix} = \Lambda\, \mathrm{i}\, \hat{\boldsymbol{e}}_k \times \begin{Bmatrix} \tilde{\boldsymbol{u}}_{\boldsymbol{k}} \\ \tilde{\boldsymbol{b}}_{\boldsymbol{k}} \end{Bmatrix}. \tag{2.20}$$

We obtain the general solution

$$\omega \equiv \omega_\Lambda^s = \frac{s k_\parallel \Omega_0}{k} \left(-s\Lambda + \sqrt{1 + k^2 d^2} \right), \tag{2.21}$$

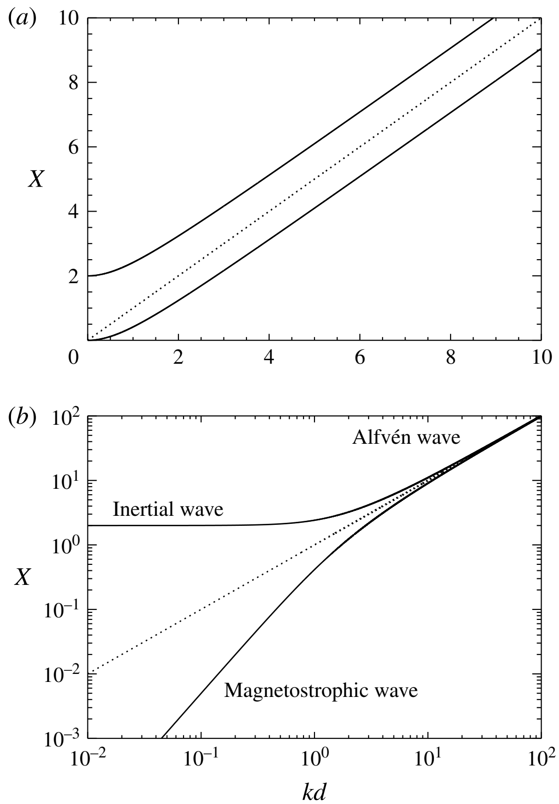

FIGURE 1. Dispersion relation for rotating MHD permeated by a background magnetic field in (*a*) linear and (*b*) logarithmic coordinates, with $X \equiv k\omega_\Lambda^s/(sk_\parallel \Omega_0)$. In each panel the upper and lower solid branches correspond, respectively, to left- and right-handed polarized waves; the Alfvén wave dispersion relation is also shown (as a dotted line).

where the value (± 1) of s defines the directional wave polarity such that we always have $sk_\parallel \geqslant 0$; then ω_Λ^s is a positive-definite pulsation. The wave polarization Λ tells us whether the wave is right ($\Lambda = s$) or left ($\Lambda = -s$) circularly polarized. In the former case we are dealing with the magnetostrophic branch, whereas in the latter case we are dealing with the inertial branch (see figure 1). We see that the transverse circularly polarized waves are dispersive and that we recover the two well-known limits, i.e. the pure inertial waves ($\omega_{-s}^s = 2s\Omega_0 k_\parallel/k \equiv \omega_I$) in the large-scale limit ($kd \to 0$) and the standard Alfvén waves ($\omega = sk_\parallel b_0 \equiv \omega_A$) in the small-scale limit ($kd \to +\infty$). For the pure magnetostrophic waves we find the pulsation, $\omega_s^s = sk_\parallel kdb_0/2 = \omega_A^2/\omega_I \equiv \omega_M$. The Alfvén waves become linearly polarized only when the Coriolis force vanishes; when it is present, whatever its magnitude, the modified Alfvén waves are circularly polarized. It is interesting to note that this property is also found in MHD when, instead of the Coriolis term, the Hall term is added to the incompressible equations (Sahraoui, Galtier & Belmont 2007).

2.4. *Polarization*

The polarizations s and Λ can be related to two well-known quantities, the reduced magnetic helicity σ^m and the reduced cross-helicity σ^c. The reduced magnetic helicity is defined as

$$\sigma^m = \frac{\boldsymbol{a_k} \cdot \boldsymbol{b}_k^* + \boldsymbol{a}_k^* \cdot \boldsymbol{b_k}}{2|\boldsymbol{a_k}|\, |\boldsymbol{b_k}|}, \tag{2.22}$$

where $*$ denotes the complex conjugate. For circularly polarized waves, we can use relation (2.20), which gives $\sigma^m = \Lambda$. On the other hand, the reduced cross-helicity is defined as

$$\sigma^c = \frac{\boldsymbol{u_k} \cdot \boldsymbol{b}_k^* + \boldsymbol{u}_k^* \cdot \boldsymbol{b_k}}{2|\boldsymbol{u_k}|\, |\boldsymbol{b_k}|}. \tag{2.23}$$

The linear solution implies $\omega \boldsymbol{b_k} = -s|k_\parallel| b_0 \boldsymbol{u_k}$, which leads to $\sigma^c = -s$. The use of both relations yields

$$\sigma^m \sigma^c = -\Lambda s. \tag{2.24}$$

This result is valid only for the linear solutions but may be generalized to any fluctuations in order to derive the properties of helical turbulence (Meyrand & Galtier 2012).

2.5. *Magnetostrophic equation*

The governing equations of rotating MHD can also be written in the following form:

$$\frac{\partial \boldsymbol{w}}{\partial t} = \nabla \times [\boldsymbol{u} \times (\boldsymbol{w} + 2\boldsymbol{\Omega}_0) + \boldsymbol{j} \times (\boldsymbol{b} + d\boldsymbol{\Omega}_0)] + \nu \nabla^2 \boldsymbol{w}, \tag{2.25}$$

$$\frac{\partial \boldsymbol{b}}{\partial t} = \nabla \times [\boldsymbol{u} \times (\boldsymbol{b} + \boldsymbol{b}_0)] + \eta \nabla^2 \boldsymbol{b}, \tag{2.26}$$

where the relation $\boldsymbol{b}_0 = d\boldsymbol{\Omega}_0$ has been introduced. The magnetostrophic regime corresponds to a balance between the Coriolis and Lorentz–Laplace forces (Finlay 2008). If we balance such terms in the linear case, we obtain the relation

$$2\boldsymbol{u} = -d\boldsymbol{j}, \tag{2.27}$$

which can be substituted into (2.26) to give

$$\frac{\partial \boldsymbol{b}}{\partial t} = -\frac{d}{2} \nabla \times [(\nabla \times \boldsymbol{b}) \times (\boldsymbol{b} + \boldsymbol{b}_0)] + \eta \nabla^2 \boldsymbol{b}. \tag{2.28}$$

Expression (2.28) is the magnetostrophic equation which describes the nonlinear evolution of the magnetic field when both the rotation and the uniform magnetic field are relatively strong. It is asymptotically true in the sense that it corresponds only to the lower part of the magnetostrophic branch shown in figure 1. We note immediately its similarity to the electron MHD equation introduced in plasma physics (Kingsep, Chukbar & Yankov 1990) to describe the small space–time evolution of a magnetized plasma. The difference resides in the coefficient $d/2$, which is the ion skin depth d_i in electron MHD. It is then not surprising that the linear solution gives the same (up to a factor of $1/2$) dispersion relation as for whistler waves, which are also right circularly polarized. We will see in § 5.6 that in the large-scale right-polarization limit the general weak turbulence equations indeed give the same equation (up to a constant factor) as in the electron MHD case (Galtier & Bhattacharjee 2003).

2.6. *Complex helicity decomposition*

Given the incompressibility constraints (2.16) and (2.17), it is convenient to project the rotating MHD equations in a plane orthogonal to $\boldsymbol{k}$. We will use the complex helicity decomposition technique, which has been shown to be effective in providing a compact description of the dynamics of three-dimensional incompressible fluids (Craya 1954; Kraichnan 1973; Waleffe 1992; Lesieur 1997; Turner 2000; Galtier 2003, 2006*b*). The complex helicity basis is also particularly useful because it allows us to diagonalize systems dealing with circularly polarized waves. We introduce the complex helicity decomposition

$$\boldsymbol{h}^{\Lambda}(\boldsymbol{k}) \equiv \boldsymbol{h}_{\boldsymbol{k}}^{\Lambda} = \hat{\boldsymbol{e}}_\theta + \mathrm{i}\Lambda \hat{\boldsymbol{e}}_\Phi, \tag{2.29}$$

where

$$\hat{\boldsymbol{e}}_\theta = \hat{\boldsymbol{e}}_\Phi \times \hat{\boldsymbol{e}}_k, \quad \hat{\boldsymbol{e}}_\Phi = \frac{\hat{\boldsymbol{e}}_\parallel \times \hat{\boldsymbol{e}}_k}{|\hat{\boldsymbol{e}}_\parallel \times \hat{\boldsymbol{e}}_k|}, \tag{2.30}$$

with $|\hat{\boldsymbol{e}}_\theta(\boldsymbol{k})| = |\hat{\boldsymbol{e}}_\Phi(\boldsymbol{k})| = 1$. We note that $(\hat{\boldsymbol{e}}_k, h_{\boldsymbol{k}}^{+}, h_{\boldsymbol{k}}^{-})$ form a complex basis with the following properties:

$$\boldsymbol{h}_{\boldsymbol{k}}^{-\Lambda} = \boldsymbol{h}_{-\boldsymbol{k}}^{\Lambda}, \tag{2.31}$$

$$\hat{\boldsymbol{e}}_k \times \boldsymbol{h}_{\boldsymbol{k}}^{\Lambda} = -\mathrm{i}\Lambda\, \boldsymbol{h}_{\boldsymbol{k}}^{\Lambda}, \tag{2.32}$$

$$\boldsymbol{k} \boldsymbol{\cdot} \boldsymbol{h}_{\boldsymbol{k}}^{\Lambda} = 0, \tag{2.33}$$

$$\boldsymbol{h}_{\boldsymbol{k}}^{\Lambda} \boldsymbol{\cdot} \boldsymbol{h}_{\boldsymbol{k}}^{\Lambda'} = 2\,\delta_{-\Lambda'\Lambda}. \tag{2.34}$$

We project the Fourier transform of the original vectors $\boldsymbol{u}(\boldsymbol{x})$ and $\boldsymbol{b}(\boldsymbol{x})$ onto the helicity basis (see also appendix B):

$$\boldsymbol{u}_{\boldsymbol{k}} = \sum_{\Lambda} \mathscr{U}_\Lambda(\boldsymbol{k})\, \boldsymbol{h}_{\boldsymbol{k}}^{\Lambda} = \sum_{\Lambda} \mathscr{U}_\Lambda\, \boldsymbol{h}_{\boldsymbol{k}}^{\Lambda}, \tag{2.35}$$

$$\boldsymbol{b}_{\boldsymbol{k}} = \sum_{\Lambda} \mathscr{B}_\Lambda(\boldsymbol{k})\, \boldsymbol{h}_{\boldsymbol{k}}^{\Lambda} = \sum_{\Lambda} \mathscr{B}_\Lambda\, \boldsymbol{h}_{\boldsymbol{k}}^{\Lambda}. \tag{2.36}$$

In particular, we note that

$$\boldsymbol{w}_{\boldsymbol{k}} = k \sum_{\Lambda} \Lambda\, \mathscr{U}_\Lambda\, \boldsymbol{h}_{\boldsymbol{k}}^{\Lambda}, \tag{2.37}$$

$$\boldsymbol{j}_{\boldsymbol{k}} = k \sum_{\Lambda} \Lambda\, \mathscr{B}_\Lambda\, \boldsymbol{h}_{\boldsymbol{k}}^{\Lambda}. \tag{2.38}$$

We substitute the expressions for the new fields into the rotating MHD equations written in Fourier space and multiply by the vector $\boldsymbol{h}_{-\boldsymbol{k}}^{\Lambda}$. First, we focus on the linear dispersion relation ($\epsilon = 0$), which reads

$$\partial_t \mathscr{Z}_\Lambda^s = -\mathrm{i}\, \omega_\Lambda^s\, \mathscr{Z}_\Lambda^s, \tag{2.39}$$

with

$$\mathscr{Z}_\Lambda^s \equiv \mathscr{U}_\Lambda + \xi_\Lambda^s \mathscr{B}_\Lambda, \tag{2.40}$$

$$\xi_\Lambda^s \equiv \frac{-skd}{-s\Lambda + \sqrt{1 + k^2 d^2}}. \tag{2.41}$$

Equation (2.39) shows that the $\mathscr{Z}_\Lambda^s$ are the canonical variables for our system. These eigenvectors combine the velocity and the magnetic field in a non-trivial way through a factor ξ_Λ^s (with $\omega_\Lambda^s = -b_0 k_\parallel/\xi_\Lambda^s$). In the small-scale limit ($kd \rightarrow +\infty$), we see that $\xi_\Lambda^s \rightarrow -s$; the Elsässer variables used in standard MHD are then recovered. In the large-scale limit ($kd \rightarrow 0$) we have $\xi_\Lambda^s \rightarrow -s\,kd/2$ for $\Lambda = -s$ (inertial waves), or $\xi_\Lambda^s \rightarrow (-2s/kd)^{-1}$ for $\Lambda = s$ (magnetostrophic waves). Therefore, $\mathscr{Z}_\Lambda^s$ can be seen as a generalization of the Elsässer variables to rotating MHD. In the rest of the paper, we shall use the relation

$$\mathscr{Z}_\Lambda^s = (\xi_\Lambda^s - \xi_\Lambda^{-s})\, a_\Lambda^s\, \mathrm{e}^{-\mathrm{i}\omega_\Lambda^s t}, \tag{2.42}$$

where a_Λ^s is the wave amplitude in the interaction representation for which we have, in the linear approximation, $\partial_t a_\Lambda^s = 0$. In particular, this means that weak nonlinearities will modify the helical MHD wave amplitudes only slowly in time. The coefficient in front of the wave amplitude is introduced in advance to simplify the algebra that we are going to develop.

3. Helical weak turbulence formalism

3.1. *Fundamental equations*

We decompose the inviscid nonlinear MHD equations (2.14) and (2.15) using the complex helicity basis introduced in the previous section. Then, we project the equations onto the vector $\boldsymbol{h}_{-\boldsymbol{k}}^{\boldsymbol{\Lambda}}$. After simplifications we obtain

$$\partial_t \mathscr{U}_\Lambda - \frac{2\mathrm{i}\Lambda\Omega_0 k_\parallel}{k}\mathscr{U}_\Lambda - \mathrm{i}b_0 k_\parallel \mathscr{B}_\Lambda = \frac{\mathrm{i}\epsilon}{2\Lambda k}\int \sum_{\Lambda_p,\Lambda_q} (p\Lambda_p - q\Lambda_q)(\mathscr{U}_{\Lambda_p}\mathscr{U}_{\Lambda_q} - \mathscr{B}_{\Lambda_p}\mathscr{B}_{\Lambda_q}) \times (\boldsymbol{q}\cdot\boldsymbol{h}_{\boldsymbol{p}}^{\Lambda_p})(\boldsymbol{h}_{\boldsymbol{q}}^{\Lambda_q}\cdot\boldsymbol{h}_{\boldsymbol{k}}^{-\Lambda})\,\delta_{pq,k}\,\mathrm{d}\boldsymbol{p}\,\mathrm{d}\boldsymbol{q} \tag{3.1}$$

and

$$\partial_t \mathscr{B}_\Lambda - \mathrm{i}b_0 k_\parallel \mathscr{U}_\Lambda = \frac{\mathrm{i}\epsilon}{2}\int \sum_{\Lambda_p,\Lambda_q} (\mathscr{U}_{\Lambda_q}\mathscr{B}_{\Lambda_p} - \mathscr{U}_{\Lambda_p}\mathscr{B}_{\Lambda_q})(\boldsymbol{q}\cdot\boldsymbol{h}_{\boldsymbol{p}}^{\Lambda_p})(\boldsymbol{h}_{\boldsymbol{q}}^{\Lambda_q}\cdot\boldsymbol{h}_{\boldsymbol{k}}^{-\Lambda})\,\delta_{pq,k}\,\mathrm{d}\boldsymbol{p}\,\mathrm{d}\boldsymbol{q}, \tag{3.2}$$

where $\delta_{pq,k} = \delta(\boldsymbol{p}+\boldsymbol{q}-\boldsymbol{k})$. The delta distributions come from the Fourier transforms of the nonlinear terms. We introduce the generalized Elsässer variables as follows:

$$\mathscr{U}_\Lambda = \sum_s \frac{-\xi_\Lambda^{-s}\mathscr{Z}_\Lambda^s}{\xi_\Lambda^s - \xi_\Lambda^{-s}}, \tag{3.3}$$

$$\mathscr{B}_\Lambda = \sum_s \frac{\mathscr{Z}_\Lambda^s}{\xi_\Lambda^s - \xi_\Lambda^{-s}}. \tag{3.4}$$

Then, in the interaction representation (the variable a_Λ^s) we have

$$\partial_t a_\Lambda^s = \frac{\mathrm{i}\epsilon}{2}\int \sum_{\substack{\Lambda_p,\Lambda_q\\ s_p,s_q}} \boldsymbol{L}_{\substack{s\,s_p\,s_q\\ -k\,p\,q}}^{\Lambda\Lambda_p\Lambda_q}\, a_{\Lambda_p}^{s_p} a_{\Lambda_q}^{s_q}\,\mathrm{e}^{-\mathrm{i}\Omega_{pq,k}t}\,\delta_{pq,k}\,\mathrm{d}\boldsymbol{p}\,\mathrm{d}\boldsymbol{q}, \tag{3.5}$$

where

$$\boldsymbol{L}_{\substack{s\,s_p\,s_q\\ k\,p\,q}}^{\Lambda\Lambda_p\Lambda_q} = \left[\left(\frac{p\Lambda_p - q\Lambda_q}{\Lambda k}\right)\left(\xi_{\Lambda_p}^{-s_p}\xi_{\Lambda_q}^{-s_q} - 1\right) + \xi_\Lambda^s\left(\xi_{\Lambda_p}^{-s_p} - \xi_{\Lambda_q}^{-s_q}\right)\right]\frac{(\boldsymbol{q}\cdot\boldsymbol{h}_{\boldsymbol{p}}^{\Lambda_p})\,(\boldsymbol{h}_{\boldsymbol{q}}^{\Lambda_q}\cdot\boldsymbol{h}_{\boldsymbol{k}}^{\Lambda})}{\xi_\Lambda^s - \xi_\Lambda^{-s}} \tag{3.6}$$

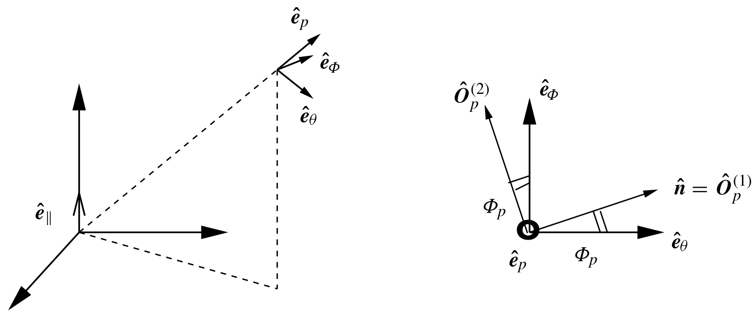

FIGURE 2. Local decomposition for a given wavevector $\boldsymbol{p}$.

and

$$\Omega_{pq,k} = \omega_{\Lambda_p}^{s_p} + \omega_{\Lambda_q}^{s_q} - \omega_{\Lambda}^{s}. \tag{3.7}$$

Equation (3.5) is the wave amplitude equation, from which it is possible to extract some information. As expected, we see that the nonlinear terms are of order ϵ. This means that weak nonlinearities will modify only slowly in time the helical MHD wave amplitude. They contain an exponentially oscillating term which is essential for the asymptotic closure. Indeed, weak turbulence deals with variations of spectral densities at very large times, i.e. for a nonlinear transfer time much greater than the wave period; in other words, we assume a time scale separation between the fast oscillations of the waves due to the phase variations in the exponential and slow variations of the wave amplitudes. As a consequence, most of the nonlinear terms are destroyed and only a few of them, namely the resonance terms (for which $\Omega_{pq,k} = 0$), survive (see e.g. Newell, Nazarenko & Biven 2001). The expression obtained for the fundamental equation (3.5) is classical in weak turbulence. The main difference between different problems is localized in the matrix $\boldsymbol{L}$, which is interpreted as a complex geometric coefficient. We will see below that the local decomposition allows us to obtain a polar form for such a coefficient, which is much easier to manipulate. From (3.5) we see that, in contrast to incompressible MHD, there is no exact solution to the nonlinear problem in incompressible rotating MHD. This difference arises from the fact that in MHD the nonlinear term involves Alfvén waves travelling only in opposite directions, whereas in rotating MHD this constraint does not exist (we have a summation over Λ and s). In other words, if one type of wave is not present in incompressible MHD, then the nonlinear term cancels, whereas in the present problem this is not the case (see e.g. Galtier *et al.* 2000).

3.2. *Local decomposition*

In order to evaluate the scalar products of complex helical vectors found in the geometric coefficient (3.6), it is convenient to introduce a vector basis local to each particular triad (Waleffe 1992; Turner 2000; Galtier 2003). For example, for a given vector $\boldsymbol{p}$, we define the orthonormal basis vectors

$$\hat{\boldsymbol{O}}^{(1)}(\boldsymbol{p}) = \hat{\boldsymbol{n}}, \tag{3.8}$$

$$\hat{\boldsymbol{O}}^{(2)}(\boldsymbol{p}) = \hat{\boldsymbol{e}}_p \times \hat{\boldsymbol{n}}, \tag{3.9}$$

$$\hat{\boldsymbol{O}}^{(3)}(\boldsymbol{p}) = \hat{\boldsymbol{e}}_p, \tag{3.10}$$

where $\hat{\boldsymbol{e}}_p = \boldsymbol{p}/|\boldsymbol{p}|$ and

$$\hat{\boldsymbol{n}} = \frac{\boldsymbol{p} \times \boldsymbol{k}}{|\boldsymbol{p} \times \boldsymbol{k}|} = \frac{\boldsymbol{q} \times \boldsymbol{p}}{|\boldsymbol{q} \times \boldsymbol{p}|} = \frac{\boldsymbol{k} \times \boldsymbol{q}}{|\boldsymbol{k} \times \boldsymbol{q}|}. \tag{3.11}$$

We see that the vector $\hat{\boldsymbol{n}}$ is normal to any vector of the triad $(\boldsymbol{k}, \boldsymbol{p}, \boldsymbol{q})$ and changes sign if $\boldsymbol{p}$ and $\boldsymbol{q}$ are interchanged, i.e. $\hat{\boldsymbol{n}}_{(\boldsymbol{k},\boldsymbol{q},\boldsymbol{p})} = -\hat{\boldsymbol{n}}_{(\boldsymbol{k},\boldsymbol{p},\boldsymbol{q})}$. Note that $\hat{\boldsymbol{n}}$ does not change under cyclic permutation, i.e. $\hat{\boldsymbol{n}}_{(\boldsymbol{k},\boldsymbol{q},\boldsymbol{p})} = \hat{\boldsymbol{n}}_{(\boldsymbol{q},\boldsymbol{p},\boldsymbol{k})} = \hat{\boldsymbol{n}}_{(\boldsymbol{p},\boldsymbol{k},\boldsymbol{q})}$. A sketch of the local decomposition is given in figure 2. We now introduce the vectors

$$\Xi^{\Lambda_p}(\boldsymbol{p}) \equiv \Xi_{\boldsymbol{p}}^{\Lambda_p} = \hat{\boldsymbol{O}}^{(1)}(\boldsymbol{p}) + \mathrm{i}\Lambda_p \hat{\boldsymbol{O}}^{(2)}(\boldsymbol{p}) \tag{3.12}$$

and define the rotation angle Φ_p so that

$$\cos \Phi_p = \hat{\boldsymbol{n}} \boldsymbol{\cdot} \hat{\boldsymbol{e}}_\theta(\boldsymbol{p}), \tag{3.13}$$

$$\sin \Phi_p = \hat{\boldsymbol{n}} \boldsymbol{\cdot} \hat{\boldsymbol{e}}_\Phi(\boldsymbol{p}). \tag{3.14}$$

The decomposition of the helicity vector $\boldsymbol{h}_{\boldsymbol{p}}^{\Lambda_p}$ in the local basis gives (with similar forms obtained for $\boldsymbol{k}$ and $\boldsymbol{q}$)

$$\boldsymbol{h}_{\boldsymbol{p}}^{\Lambda_p} = \Xi_{\boldsymbol{p}}^{\Lambda_p} \, \mathrm{e}^{\mathrm{i}\Lambda_p \Phi_p}. \tag{3.15}$$

After some algebra we obtain the following polar form for the matrix $\boldsymbol{L}$:

$$\begin{aligned} \boldsymbol{L}\,{}^{\Lambda \Lambda_p \Lambda_q}_{\substack{s\, s_p\, s_q \\ k\, p\, q}} = & -\left[\left(\frac{p\Lambda_p - q\Lambda_q}{\Lambda k}\right)\left(\xi_{\Lambda_p}^{-s_p}\xi_{\Lambda_q}^{-s_q} - 1\right) + \xi_\Lambda^s \left(\xi_{\Lambda_p}^{-s_p} - \xi_{\Lambda_q}^{-s_q}\right)\right] \\ & \times \mathrm{i}\mathrm{e}^{\mathrm{i}(\Lambda\Phi_k + \Lambda_p\Phi_p + \Lambda_q\Phi_q)} \frac{\Lambda\, \Lambda_p\, \Lambda_q}{\xi_\Lambda^s - \xi_\Lambda^{-s}} \frac{\sin \psi_k}{k} kq\, (\Lambda\Lambda_q + \cos\psi_p). \end{aligned} \tag{3.16}$$

The angle ψ_k refers to the angle opposite $\boldsymbol{k}$ in the triangle defined by $\boldsymbol{k} = \boldsymbol{p} + \boldsymbol{q}$ ($\sin \psi_k = \hat{\boldsymbol{n}} \cdot (\boldsymbol{q} \times \boldsymbol{p})/|(\boldsymbol{q} \times \boldsymbol{p})|$). To obtain (3.16), we have also used the well-known triangle relations

$$\frac{\sin \psi_k}{k} = \frac{\sin \psi_p}{p} = \frac{\sin \psi_q}{q}. \tag{3.17}$$

Further modifications are needed before we can apply the spectral formalism. In particular, the fundamental equation has to be invariant under interchange of $\boldsymbol{p}$ and $\boldsymbol{q}$. To ensure this, we introduce the symmetrized matrix

$$\frac{1}{2}\left(\boldsymbol{L}\,{}^{\Lambda \Lambda_p \Lambda_q}_{\substack{s\, s_p\, s_q \\ k\, p\, q}} + \boldsymbol{L}\,{}^{\Lambda \Lambda_q \Lambda_p}_{\substack{s\, s_q\, s_p \\ k\, q\, p}}\right). \tag{3.18}$$

Finally, by using the identities given in appendix A, we obtain

$$\partial_t a_\Lambda^s = \frac{\epsilon\, d^2}{16} \int \sum_{\substack{\Lambda_p, \Lambda_q \\ s_p, s_q}} \frac{\xi_{\Lambda_q}^{-s_q} - \xi_{\Lambda_p}^{-s_p}}{\xi_\Lambda^s - \xi_\Lambda^{-s}} \boldsymbol{M}\,{}^{\Lambda \Lambda_p \Lambda_q}_{\substack{s\, s_p\, s_q \\ -k\, p\, q}} a_{\Lambda_p}^{s_p} a_{\Lambda_q}^{s_q} \, \mathrm{e}^{-\mathrm{i}\Omega_{pq,k} t} \, \delta_{pq,k} \, \mathrm{d}\boldsymbol{p} \, \mathrm{d}\boldsymbol{q}, \tag{3.19}$$

where

$$\boldsymbol{M}\,{}^{\Lambda\Lambda_p\Lambda_q}_{\;s\,s_p\,s_q}_{\;k\,p\,q} = \mathrm{e}^{\mathrm{i}(\Lambda\Phi_k+\Lambda_p\Phi_p+\Lambda_q\Phi_q)}\,(\Lambda k+\Lambda_p p+\Lambda_q q)kpq\frac{\sin\psi_k}{k}\xi^s_\Lambda\xi^{s_p}_{\Lambda_p}\xi^{s_q}_{\Lambda_q}$$
$$\times\left(2+(\xi^{-s}_\Lambda)^2(\xi^{-s_p}_{\Lambda_p})^2(\xi^{-s_q}_{\Lambda_q})^2-(\xi^{-s}_\Lambda)^2-(\xi^{-s_p}_{\Lambda_p})^2-(\xi^{-s_q}_{\Lambda_q})^2\right). \quad (3.20)$$

The matrix $\boldsymbol{M}$ possesses the following properties:

$$\left(\boldsymbol{M}\,{}^{\Lambda\Lambda_p\Lambda_q}_{\;s\,s_p\,s_q}_{\;k\,p\,q}\right)^* = \boldsymbol{M}\,{}^{-\Lambda-\Lambda_p-\Lambda_q}_{\;-s\,-s_p\,-s_q}_{\;k\;p\;q} = \boldsymbol{M}\,{}^{\Lambda\;\Lambda_p\;\Lambda_q}_{\;s\;s_p\;s_q}_{\;-k\,-p\,-q}, \quad (3.21)$$

$$\boldsymbol{M}\,{}^{\Lambda\Lambda_p\Lambda_q}_{\;s\,s_p\,s_q}_{\;k\,p\,q} = -\boldsymbol{M}\,{}^{\Lambda\Lambda_q\Lambda_p}_{\;s\,s_q\,s_p}_{\;k\,q\,p}, \quad (3.22)$$

$$\boldsymbol{M}\,{}^{\Lambda\Lambda_p\Lambda_q}_{\;s\,s_p\,s_q}_{\;k\,p\,q} = -\boldsymbol{M}\,{}^{\Lambda_q\Lambda_p\Lambda}_{\;s_q\,s_p\,s}_{\;q\,p\,k}, \quad (3.23)$$

$$\boldsymbol{M}\,{}^{\Lambda\Lambda_p\Lambda_q}_{\;s\,s_p\,s_q}_{\;k\,p\,q} = -\boldsymbol{M}\,{}^{\Lambda_p\Lambda\Lambda_q}_{\;s_p\,s\,s_q}_{\;p\,k\,q}. \quad (3.24)$$

Equation (3.19) is the fundamental equation that describes the slow evolution of the wave amplitudes due to the nonlinear terms of the incompressible rotating MHD equations. It is the starting point for deriving the weak turbulence equations. The local decomposition used here allows us to represent complex information concisely in an exponential function (polar form). As we will see below, this representation simplifies significantly the derivation of the asymptotic equations.

From (3.19), we note that the nonlinear coupling between helicity states associated with the wavevectors $\boldsymbol{p}$ and $\boldsymbol{q}$ vanishes when the wavevectors are collinear (because then $\sin\psi_k=0$). This property is similar to one found for pure rotating hydrodynamics. It seems to be a general property of helical waves (Kraichnan 1973; Waleffe 1992; Turner 2000; Galtier 2003, 2006*b*). Additionally, we note that the nonlinear coupling between helicity states vanishes whenever the wavenumbers p and q are equal, if their associated wave and directional polarities (Λ_p, Λ_q and s_p, s_q, respectively) are also equal. In the case of inertial waves, for which we have $\Lambda=-s$ (left-handed waves), this property was already observed (Galtier 2003). Here, this finding is generalized to right and left circularly polarized waves. Note that in the large-scale limit for which we recover the linearly polarized Alfvén waves, this property tends to disappear (see also § 5.4).

We are interested in the long-time behaviour of the helical wave amplitudes. From the fundamental equation (3.19), we see that the nonlinear wave coupling will come from resonant terms such that

$$\begin{cases} \boldsymbol{k}=\boldsymbol{p}+\boldsymbol{q}, \\ \dfrac{k_\parallel}{\xi^s_\Lambda}=\dfrac{p_\parallel}{\xi^{s_p}_{\Lambda_p}}+\dfrac{q_\parallel}{\xi^{s_q}_{\Lambda_q}}. \end{cases} \quad (3.25)$$

The resonance condition may also be written as

$$\frac{\xi^{-s}_\Lambda-\xi^{-s_p}_{\Lambda_p}}{q_\parallel}=\frac{\xi^{-s_q}_{\Lambda_q}-\xi^{-s}_\Lambda}{p_\parallel}=\frac{\xi^{-s_q}_{\Lambda_q}-\xi^{-s_p}_{\Lambda_p}}{k_\parallel}. \quad (3.26)$$

As we shall see below, relations (3.26) are useful in simplifying the weak turbulence equations and demonstrating the conservation of inviscid invariants.

3.3. *Asymptotic weak turbulence equations*

Weak turbulence is a state of a system composed of many simultaneously excited and interacting nonlinear waves where the energy distribution, far from thermodynamic equilibrium (Zakharov *et al.* 1992), is characterized by a wide power-law spectrum. This range of wavenumbers – the inertial range – is generally localized between large scales at which energy is injected into the system and small dissipative scales. The origin of weak turbulence dates back to the early 1960s, and since then many papers have been devoted to the subject (see e.g. Hasselmann 1962; Benney & Saffman 1966; Zakharov 1967; Sagdeev & Galeev 1969; Kuznetsov 1972; Zakharov *et al.* 1992; Galtier 2009*b*; Nazarenko 2011). The essence of weak turbulence is the statistical study of large ensembles of weakly interacting dispersive waves via a systematic asymptotic expansion in powers of the small nonlinearity. This technique leads to the derivation of kinetic equations for quantities such as the energy and, more generally, the (quadratic) invariants of the system under investigation. Here, we will follow the standard Eulerian formalism of weak turbulence (see e.g. Benney & Newell 1969).

We define the density tensor $\boldsymbol{q}^s_\Lambda(\boldsymbol{k})$ for a homogeneous turbulence, such that

$$\langle a^s_\Lambda(\boldsymbol{k})\, a^{s'}_{\Lambda'}(\boldsymbol{k}')\rangle \equiv \boldsymbol{q}^s_\Lambda(\boldsymbol{k})\, \delta(\boldsymbol{k}+\boldsymbol{k}')\, \delta_{\Lambda\Lambda'}\, \delta_{ss'}, \tag{3.27}$$

for which we shall write an asymptotic closure equation. The presence of the deltas $\delta_{\Lambda\Lambda'}$ and $\delta_{ss'}$ means that correlations with opposite wave or directional polarities have no long-time influence in the wave turbulence regime; the third delta distribution $\delta(\boldsymbol{k}+\boldsymbol{k}')$ is a consequence of the homogeneity assumption. Details of the derivation of the weak turbulence equations (which include the dissipative terms) are given in appendix C. After a lengthy calculation, we obtain the following result:

$$\begin{aligned}\partial_t \boldsymbol{q}^s_\Lambda(\boldsymbol{k}) = {} & \frac{\pi\,\epsilon^2 d^4}{64\, b_0^2} \int \sum_{\substack{\Lambda_p,\Lambda_q\\ s_p,s_q}} \left(\frac{\sin\psi_k}{k}\right)^2 k^2p^2q^2(\Lambda k+\Lambda_p p+\Lambda_q q)^2(\xi^s_\Lambda)^2(\xi^{s_p}_{\Lambda_p})^2(\xi^{s_q}_{\Lambda_q})^2 \\ & \times \left(\frac{\xi^{-s_q}_{\Lambda_q}-\xi^{-s_p}_{\Lambda_p}}{k_\parallel}\right)^2 \left(2+(\xi^{-s}_\Lambda)^2(\xi^{-s_p}_{\Lambda_p})^2(\xi^{-s_q}_{\Lambda_q})^2-(\xi^{-s}_\Lambda)^2-(\xi^{-s_p}_{\Lambda_p})^2-(\xi^{-s_q}_{\Lambda_q})^2\right)^2 \\ & \times \left(\frac{\omega^s_\Lambda}{1+(\xi^{-s}_\Lambda)^2}\right) \boldsymbol{q}^s_\Lambda(\boldsymbol{k})\, \boldsymbol{q}^{s_p}_{\Lambda_p}(\boldsymbol{p})\, \boldsymbol{q}^{s_q}_{\Lambda_q}(\boldsymbol{q}) \\ & \times \left[\frac{\omega^s_\Lambda}{\{1+(\xi^{-s}_\Lambda)^2\}\boldsymbol{q}^s_\Lambda(\boldsymbol{k})}-\frac{\omega^{s_p}_{\Lambda_p}}{\{1+(\xi^{-s_p}_{\Lambda_p})^2\}\boldsymbol{q}^{s_p}_{\Lambda_p}(\boldsymbol{p})}-\frac{\omega^{s_q}_{\Lambda_q}}{\{1+(\xi^{-s_q}_{\Lambda_q})^2\}\boldsymbol{q}^{s_q}_{\Lambda_q}(\boldsymbol{q})}\right] \\ & \times \delta(\Omega_{k,pq})\, \delta_{k,pq}\, \mathrm{d}\boldsymbol{p}\, \mathrm{d}\boldsymbol{q}.\end{aligned} \tag{3.28}$$

Equation (3.28) is the main result of the helical weak turbulence formalism. It describes the statistical properties of weak turbulence for rotating MHD at the lowest order, i.e. for three-wave interactions.

4. Phenomenology of the weak turbulence dynamo

Before going into the detailed analysis of the weak turbulence regime, it is important to have a simple picture in mind of the physical process that we are going to describe. According to the properties given in § 3.2, if we assume that the

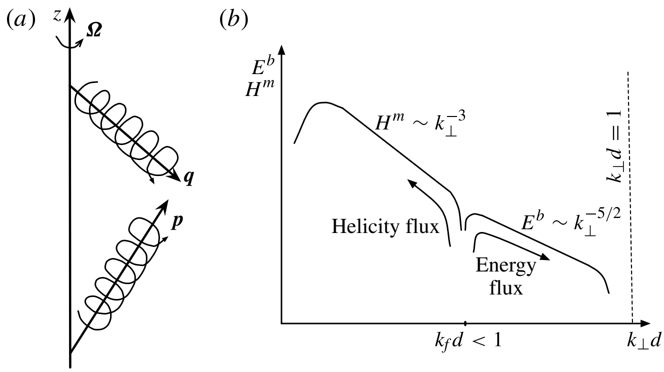

FIGURE 3. (*a*) Collision between counterpropagating circularly polarized waves. (*b*) Heuristic view of the magnetic energy and hybrid helicity spectra with a forcing applied at an intermediate scale $k_f d < 1$; the inverse cascade of helicity can drive the energy to the largest scales of the system. We do not consider the case where the inertial ranges satisfy the condition $k_\perp d > 1$, which corresponds to pure weak Alfvén wave turbulence.

nonlinear transfer is mainly driven by local interactions ($k \sim p \sim q$), then we can consider only stochastic collisions between counterpropagating waves (Iroshnikov 1964; Kraichnan 1965) of the same kind to derive the form of the energy spectra (see figure 3); in other words, a left-handed (respectively, right-handed) wave going upward will interact much more strongly with another left-handed (respectively, right-handed) wave propagating downward than with one going upward.

To find the transfer time and then the energy spectrum, we first need to evaluate the modification of a wave produced by one collision. Starting from the momentum equation (for simplicity we write the wave amplitude as $\mathscr{Z}_\ell$ and assume anisotropy with $k \sim k_\perp$), we have

$$\mathscr{Z}_\ell(t+\tau_1) \sim \mathscr{Z}_\ell(t) + \tau_1 \frac{\partial \mathscr{Z}_\ell}{\partial t} \sim \mathscr{Z}_\ell(t) + \tau_1 \frac{\mathscr{Z}_\ell^2}{\ell_\perp}, \tag{4.1}$$

where τ_1 is the duration of one collision; in other words, after one collision the distortion of a wave is $\Delta_1 \mathscr{Z}_\ell \sim \tau_1 \mathscr{Z}_\ell^2/\ell_\perp$. This distortion is going to increase with time in such a way that after N stochastic collisions the cumulative effect may be evaluated like a random walk:

$$\sum_{i=1}^{N} \Delta_i \mathscr{Z}_\ell \sim \tau_1 \frac{\mathscr{Z}_\ell^2}{\ell_\perp} \sqrt{\frac{t}{\tau_1}}. \tag{4.2}$$

The transfer time, τ_{tr}, that we are looking for is the time for which the cumulative distortion is of order 1, i.e. of the order of the wave itself:

$$\mathscr{Z}_\ell \sim \tau_1 \frac{\mathscr{Z}_\ell^2}{\ell_\perp} \sqrt{\frac{\tau_{tr}}{\tau_1}}. \tag{4.3}$$

Then we obtain

$$\tau_{tr} \sim \frac{1}{\tau_1} \frac{\ell_\perp^2}{\mathscr{Z}_\ell^2} \sim \frac{\tau_{NL}^2}{\tau_1}. \tag{4.4}$$

This is basically the formula that we are going to use to evaluate the energy spectra. Let us consider inertial waves for which $\tau_1 \sim 1/\omega_I$. A classical calculation, with $\varepsilon^u \sim \mathscr{Z}_\ell^2/\tau_{tr}$, leads finally to the bi-dimensional axisymmetric kinetic energy spectrum

$$E^u(k_\perp, k_\parallel) \sim \sqrt{\varepsilon^u \varOmega_0}\, k_\perp^{-5/2} k_\parallel^{-1/2}, \tag{4.5}$$

which is the prediction for weak inertial wave turbulence (Galtier 2003). Note that this solution corresponds to a constant kinetic energy flux ε^u, whereas a constant kinetic helicity flux may give other solutions (Galtier 2014). For magnetostrophic waves we have $\tau_1 \sim 1/\omega_M$, but a subtlety arises because, instead of the momentum equation, we now use (2.28) for which the nonlinear term leads to $\tau_{NL} \sim \ell_\perp^2/(d\mathscr{Z}_\ell)$. Then, we obtain the bi-dimensional axisymmetric magnetic energy spectrum

$$E^b(k_\perp, k_\parallel) \sim \sqrt{\frac{\varepsilon^b b_0}{d}}\, k_\perp^{-5/2} k_\parallel^{-1/2}, \tag{4.6}$$

which corresponds to a constant magnetic energy flux ε^b solution.

The same heuristic analysis can be done for the other invariant, the hybrid helicity. Let us consider the most interesting case, namely the magnetostrophic regime in which the hybrid helicity is dominated by the magnetic helicity (with $kd < 1$). By using the transfer time derived above (with the helicity flux $\tilde{\varepsilon} \sim H_\ell/\tau_{tr}$), we find that

$$H(k_\perp, k_\parallel) \sim H^m(k_\perp, k_\parallel) \sim \sqrt{\frac{\tilde{\varepsilon} b_0}{d^2}}\, k_\perp^{-3} k_\parallel^{-1/2}. \tag{4.7}$$

An inverse cascade may occur for the hybrid helicity (see figure 3), which in turn can drive the magnetic energy at the largest scales of the system. It is through this mechanism that the large-scale magnetic field can be regenerated by the weak turbulence dynamo. It is important to keep in mind that this cascade happens because the hybrid helicity is an inviscid and ideal invariant (in turbulence a cascade mechanism can only happen for the inviscid invariants of a fluid; see Frisch 1995) of rotating MHD; for example, without rotation an inverse cascade of magnetic helicity is impossible in weak incompressible MHD turbulence (Galtier & Nazarenko 2008), and in pure three-dimensional incompressible hydrodynamics the cascade mechanism applies only to the kinetic energy and the kinetic helicity, which are both inviscid invariants. In other words, the inverse cascade should stop as soon as the mean magnetic field and the rotation rate are not collinear anymore (see also the discussion about the inviscid invariants in § 2.2). It is likely, however, that the inverse cascade is only weakly reduced when the mean magnetic field and the rotation rate become slightly out of alignment (weak tilt case) and is completely inhibited in the strong tilt case (because the hybrid helicity is still roughly conserved in the former case but clearly not conserved in the latter case). This comment might explain why planetary magnetic fields are often dipolar with a weak tilt ($<10^\circ$) of the dipole relative to the rotation axis. We recall that in our approach the uniform magnetic field $\boldsymbol{b}_0$ can be interpreted as the dipolar external magnetic field of a planet that we need to regenerate by a dynamo process. Also, the inverse cascade at a planetary scale would correspond to the successive nonlinear excitation of magnetic modes whose wavelengths increase with the cascade to finally reach the wavelength of the dipolar magnetic field. This scenario seems to be acceptable for planets like Earth, Jupiter or Saturn, but not for Uranus and Neptune, where a large angle exists between the rotation axis and the large-scale magnetic field, which is not a dipole. The origin of this difference is still unclear but could be attributed to the internal geometry of Uranus and Neptune, which is likely to be more complex than that of the other three planets (Stanley & Bloxham 2006). In particular, if the MHD fluid is confined to a thin layer instead of a thick layer, then the homogeneity assumption and therefore the present theory become less relevant. As we shall see, the increase of the magnetic field at large scales can lead to a state where the ratio between the magnetic and kinetic energies is significantly greater than 1. This situation is very different from the pure MHD case (i.e. without the Coriolis force), where an equipartition is found in the weak turbulence regime (Galtier *et al.* 2000).

5. General properties

In this section we present the general properties of the weak turbulence equations (3.28). We also write the simplified form of (3.28) in the three relevant limits of Alfvén, inertial and magnetostrophic waves in order to demonstrate the compatibility with previous works. This last point is particularly important as the derivation is long and non-trivial; also, it can be seen as a verification or check of the calculation.

5.1. *Basic turbulent spectra*

In § 2.2 we introduced the three-dimensional inviscid invariants of incompressible rotating MHD. The first test that the weak turbulence equations have to pass is the detailed conservation of these invariants, that is to say, the conservation of invariants for each triad $(\boldsymbol{k}, \boldsymbol{p}, \boldsymbol{q})$. Starting from the definitions (2.8) and (2.9), we find the total energy spectrum

$$E(\boldsymbol{k}) = \sum_{\Lambda,s} \{1 + (\xi_\Lambda^{-s})^2\}\, \boldsymbol{q}_\Lambda^s(\boldsymbol{k}) \equiv \sum_{\Lambda,s} \mathscr{E}_\Lambda^s(\boldsymbol{k}), \tag{5.1}$$

which is composed of the magnetic spectrum,

$$E^b(\boldsymbol{k}) = \sum_{\Lambda,s} \boldsymbol{q}_\Lambda^s(\boldsymbol{k}), \tag{5.2}$$

and the kinetic spectrum,

$$E^u(\boldsymbol{k}) = \sum_{\Lambda,s} (\xi_\Lambda^{-s})^2\, \boldsymbol{q}_\Lambda^s(\boldsymbol{k}). \tag{5.3}$$

We also find the cross-helicity spectrum

$$H^c(\boldsymbol{k}) = -\sum_{\Lambda,s} \xi_\Lambda^{-s}\, \boldsymbol{q}_\Lambda^s(\boldsymbol{k}) \tag{5.4}$$

and the magnetic helicity spectrum

$$H^m(\boldsymbol{k}) = \sum_{\Lambda,s} \frac{\Lambda}{k}\, \boldsymbol{q}_\Lambda^s(\boldsymbol{k}). \tag{5.5}$$

Note that each of these spectra may be decomposed into right ($\Lambda = s$) and left ($\Lambda = -s$) polarization spectra. From the last two expressions we find the second inviscid invariant, the hybrid helicity spectrum

$$H(\boldsymbol{k}) = \sum_{\Lambda,s} \left(\frac{\xi_\Lambda^s - \xi_\Lambda^{-s}}{2} \right) \boldsymbol{q}_\Lambda^s(\boldsymbol{k}) \equiv \sum_{\Lambda,s} \mathscr{H}_\Lambda^s(\boldsymbol{k}). \tag{5.6}$$

Below we shall demonstrate conservation of the energy and the hybrid helicity.

5.2. *Triadic conservation of inviscid invariants*

We will first check the energy conservation. From expression (3.28) we may write

$$\begin{aligned} \partial_t E(t) &\equiv \partial_t \int E(\boldsymbol{k})\, \mathrm{d}\boldsymbol{k} \equiv \partial_t \int \sum_{\Lambda,s} \mathscr{E}_\Lambda^s(\boldsymbol{k})\, \mathrm{d}\boldsymbol{k} \\ &= \frac{\pi\, \epsilon^2 d^4}{64\, b_0^2} \int \sum_{\substack{\Lambda,\Lambda_p,\Lambda_q \\ s,s_p,s_q}} \left(\frac{\sin\psi_k}{k} \right)^2 k^2 p^2 q^2 (\Lambda k + \Lambda_p p + \Lambda_q q)^2 (\xi_\Lambda^s)^2 (\xi_{\Lambda_p}^{s_p})^2 (\xi_{\Lambda_q}^{s_q})^2 \\ &\quad \times \left(\frac{\xi_{\Lambda_q}^{-s_q} - \xi_{\Lambda_p}^{-s_p}}{k_\parallel} \right)^2 \left(2 + (\xi_\Lambda^{-s})^2 (\xi_{\Lambda_p}^{-s_p})^2 (\xi_{\Lambda_q}^{-s_q})^2 - (\xi_\Lambda^{-s})^2 - (\xi_{\Lambda_p}^{-s_p})^2 - (\xi_{\Lambda_q}^{-s_q})^2 \right)^2 \\ &\quad \times \boldsymbol{q}_\Lambda^s(\boldsymbol{k}) \boldsymbol{q}_{\Lambda_p}^{s_p}(\boldsymbol{p})\, \boldsymbol{q}_{\Lambda_q}^{s_q}(\boldsymbol{q})\, \omega_\Lambda^s \left[\frac{\omega_\Lambda^s}{\mathscr{E}_\Lambda^s(\boldsymbol{k})} + \frac{\omega_{\Lambda_p}^{s_p}}{\mathscr{E}_{\Lambda_p}^{s_p}(\boldsymbol{p})} + \frac{\omega_{\Lambda_q}^{s_q}}{\mathscr{E}_{\Lambda_q}^{s_q}(\boldsymbol{q})} \right] \delta(\Omega_{kpq})\, \delta_{kpq}\, \mathrm{d}\boldsymbol{k}\, \mathrm{d}\boldsymbol{p}\, \mathrm{d}\boldsymbol{q}. \end{aligned} \tag{5.7}$$

This equation describes the time variation of the total energy of the system in the inviscid case. As this quantity is an inviscid invariant, we expect to get no variation in time. Equation (5.7) is invariant under cyclic permutations of wavevectors; it leads to

$$\begin{aligned} \partial_t E(t) &= \frac{\pi\, \epsilon^2 d^4}{192\, b_0^2} \int \sum_{\substack{\Lambda,\Lambda_p,\Lambda_q \\ s,s_p,s_q}} \left(\frac{\sin\psi_k}{k} \right)^2 k^2 p^2 q^2 (\Lambda k + \Lambda_p p + \Lambda_q q)^2 (\xi_\Lambda^s)^2 (\xi_{\Lambda_p}^{s_p})^2 (\xi_{\Lambda_q}^{s_q})^2 \\ &\quad \times \left(\frac{\xi_{\Lambda_q}^{-s_q} - \xi_{\Lambda_p}^{-s_p}}{k_\parallel} \right)^2 \left(2 + (\xi_\Lambda^{-s})^2 (\xi_{\Lambda_p}^{-s_p})^2 (\xi_{\Lambda_q}^{-s_q})^2 - (\xi_\Lambda^{-s})^2 - (\xi_{\Lambda_p}^{-s_p})^2 - (\xi_{\Lambda_q}^{-s_q})^2 \right)^2 \\ &\quad \times \boldsymbol{q}_\Lambda^s(\boldsymbol{k})\, \boldsymbol{q}_{\Lambda_p}^{s_p}(\boldsymbol{p})\, \boldsymbol{q}_{\Lambda_q}^{s_q}(\boldsymbol{q})\, \Omega_{kpq} \left[\frac{\omega_\Lambda^s}{\mathscr{E}_\Lambda^s(\boldsymbol{k})} + \frac{\omega_{\Lambda_p}^{s_p}}{\mathscr{E}_{\Lambda_p}^{s_p}(\boldsymbol{p})} + \frac{\omega_{\Lambda_q}^{s_q}}{\mathscr{E}_{\Lambda_q}^{s_q}(\boldsymbol{q})} \right] \\ &\quad \times \delta(\Omega_{kpq})\, \delta_{kpq}\, \mathrm{d}\boldsymbol{k}\, \mathrm{d}\boldsymbol{p}\, \mathrm{d}\boldsymbol{q}. \end{aligned} \tag{5.8}$$

As we can see, with the presence of delta functions, we must consider the case where $\Omega_{kpq} = 0$, which corresponds (using the relation $\boldsymbol{k} + \boldsymbol{p} + \boldsymbol{q} = \boldsymbol{0}$) to the resonance condition (see also the discussion in § 3.1). Since the equation depends linearly on Ω_{kpq}, the total energy is conserved exactly for each triad: we have detailed conservation of the total energy.

For the second invariant, it is straightforward to show using relation (A 3) that

$$
\begin{aligned}
\partial_t H(t) &\equiv \partial_t \int H(\boldsymbol{k})\,\mathrm{d}\boldsymbol{k} \equiv \partial_t \int \sum_{\Lambda,s} \mathscr{H}^s_\Lambda(\boldsymbol{k})\,\mathrm{d}\boldsymbol{k} \\
&= \frac{\pi\,\epsilon^2 d^4}{64\, b_0^2} \int \sum_{\substack{\Lambda,\Lambda_p,\Lambda_q\\ s,s_p,s_q}} \left(\frac{\sin\psi_k}{k}\right)^2 k^2p^2q^2(\Lambda k+\Lambda_p p+\Lambda_q q)^2 (\xi^s_\Lambda)^2(\xi^{s_p}_{\Lambda_p})^2(\xi^{s_q}_{\Lambda_q})^2 \\
&\quad \times \left(\frac{\xi^{-s_q}_{\Lambda_q}-\xi^{-s_p}_{\Lambda_p}}{k_\parallel}\right)^2 \left(2+(\xi^{-s}_\Lambda)^2(\xi^{-s_p}_{\Lambda_p})^2(\xi^{-s_q}_{\Lambda_q})^2-(\xi^{-s}_\Lambda)^2-(\xi^{-s_p}_{\Lambda_p})^2-(\xi^{-s_q}_{\Lambda_q})^2\right)^2 \\
&\quad \times \boldsymbol{q}^s_\Lambda(\boldsymbol{k})\,\boldsymbol{q}^{s_p}_{\Lambda_p}(\boldsymbol{p})\,\boldsymbol{q}^{s_q}_{\Lambda_q}(\boldsymbol{q}) \frac{\xi^s_\Lambda}{2}\omega^s_\Lambda \left[\frac{2\xi^s_\Lambda\omega^s_\Lambda}{\mathscr{H}^s_\Lambda(\boldsymbol{k})}+\frac{2\xi^{s_p}_{\Lambda_p}\omega^{s_p}_{\Lambda_p}}{\mathscr{H}^{s_p}_{\Lambda_p}(\boldsymbol{p})}+\frac{2\xi^{s_q}_{\Lambda_q}\omega^{s_q}_{\Lambda_q}}{\mathscr{H}^{s_q}_{\Lambda_q}(\boldsymbol{q})}\right] \\
&\quad \times \delta(\Omega_{kpq})\,\delta_{kpq}\,\mathrm{d}\boldsymbol{k}\,\mathrm{d}\boldsymbol{p}\,\mathrm{d}\boldsymbol{q}.
\end{aligned} \tag{5.9}
$$

Equation (5.9) describes the time variation of the hybrid helicity of the system in the inviscid case. Since it is an inviscid invariant, we expect no time variation. This equation is also invariant under cyclic permutations of wavevectors. Then, one is led to

$$
\begin{aligned}
\partial_t H(t) &= \frac{\pi\,\epsilon^2 d^4}{192} \int \sum_{\substack{\Lambda,\Lambda_p,\Lambda_q\\ s,s_p,s_q}} \left(\frac{\sin\psi_k}{k}\right)^2 k^2p^2q^2(\Lambda k+\Lambda_p p+\Lambda_q q)^2 (\xi^s_\Lambda)^2(\xi^{s_p}_{\Lambda_p})^2(\xi^{s_q}_{\Lambda_q})^2 \\
&\quad \times \left(\frac{\xi^{-s_q}_{\Lambda_q}-\xi^{-s_p}_{\Lambda_p}}{k_\parallel}\right)^2 \left(2+(\xi^{-s}_\Lambda)^2(\xi^{-s_p}_{\Lambda_p})^2(\xi^{-s_q}_{\Lambda_q})^2-(\xi^{-s}_\Lambda)^2-(\xi^{-s_p}_{\Lambda_p})^2-(\xi^{-s_q}_{\Lambda_q})^2\right)^2 \\
&\quad \times \boldsymbol{q}^s_\Lambda(\boldsymbol{k})\,\boldsymbol{q}^{s_p}_{\Lambda_p}(\boldsymbol{p})\,\boldsymbol{q}^{s_q}_{\Lambda_q}(\boldsymbol{q})(k_\parallel+p_\parallel+q_\parallel) \left[\frac{k_\parallel}{\mathscr{H}^s_\Lambda(\boldsymbol{k})}+\frac{p_\parallel}{\mathscr{H}^{s_p}_{\Lambda_p}(\boldsymbol{p})}+\frac{q_\parallel}{\mathscr{H}^{s_q}_{\Lambda_q}(\boldsymbol{q})}\right] \\
&\quad \times \delta(\Omega_{kpq})\,\delta_{kpq}\,\mathrm{d}\boldsymbol{k}\,\mathrm{d}\boldsymbol{p}\,\mathrm{d}\boldsymbol{q},
\end{aligned} \tag{5.10}
$$

which is exactly equal to zero because of the resonance condition and cancellation of the term $k_\parallel + p_\parallel + q_\parallel$. Thus, we have the triadic conservation of the hybrid helicity.

5.3. *Helical properties*

From the weak turbulence equations (3.28), we deduce several general properties. Some of them can be obtained directly from the wave amplitude equation (3.19), as explained in § 3.2. First, we observe that there is no coupling between helical waves associated with wavevectors $\boldsymbol{p}$ and $\boldsymbol{q}$ when the wavevectors are collinear ($\sin\psi_k = 0$), which means that this type of wave interaction does not contribute to the (direct or inverse) cascade mechanism. Second, we note that there is no coupling between helical waves associated with vectors $\boldsymbol{p}$ and $\boldsymbol{q}$ whenever their magnitudes p and q are equal, if their associated polarities, s_p and s_q on the one hand and Λ_p and Λ_q on the other, are also equal (since then $\xi^{-s_q}_{\Lambda_q} - \xi^{-s_p}_{\Lambda_p} = 0$). Physically, this means that the strongly local interactions between two helical waves of the same kind cannot contribute significantly to the cascade. In particular, if we excite a wavepacket, the cascade mechanism will be triggered by non-local self-interactions. This property holds for the inviscid invariants and generalizes what was found previously for rotating hydrodynamics (Galtier 2003), where one only has left circularly polarized waves ($\Lambda = -s$). It seems to be a generic property of helical wave interactions (Kraichnan 1973; Waleffe 1992; Turner 2000). As noted before, this property tends to disappear when the large-scale limit is taken, i.e. when we tend to the standard MHD. Third, it follows from the previous observations that a strong helical perturbation localized initially in a narrow band of wavenumbers will lead to a weak transfer of total energy and hybrid helicities. Note that these properties can be inferred from the fundamental equation (3.19) as well.

5.4. *Small-scale dynamics: Alfvén waves*

We start with the general weak turbulence equation (3.28) and take the small-scale limit ($kd \to +\infty$), for which we have, at leading order,

$$\xi_\Lambda^s \to -s, \tag{5.11}$$

$$\left(\xi_{\Lambda_q}^{-s_q} - \xi_{\Lambda_p}^{-s_p}\right)^2 \to (s_q - s_p)^2, \tag{5.12}$$

$$\left(2 + (\xi_\Lambda^{-s})^2(\xi_{\Lambda_p}^{-s_p})^2(\xi_{\Lambda_q}^{-s_q})^2 - (\xi_\Lambda^{-s})^2 - (\xi_{\Lambda_p}^{-s_p})^2 - (\xi_{\Lambda_q}^{-s_q})^2\right)^2 \to \frac{16}{d^4}\left(\frac{s\Lambda k + s_p\Lambda_p p + s_q\Lambda_q q}{kpq}\right)^2, \tag{5.13}$$

$$\omega_\Lambda^s \to s k_\parallel b_0 = \omega_A. \tag{5.14}$$

After substituting the above expressions into (3.28), we obtain

$$\begin{aligned}\partial_t \boldsymbol{q}_\Lambda^s(\boldsymbol{k}) = {} & \frac{\pi\,\epsilon^2}{16\,b_0}\int \sum_{\substack{\Lambda_p,\Lambda_q\\ s_p,s_q}} \left(\frac{\sin\psi_k}{k}\right)^2 (\Lambda k + \Lambda_p p + \Lambda_q q)^2 \left(\frac{s_q - s_p}{k_\parallel}\right)^2 \\ & \times \left(s\Lambda k + s_p\Lambda_p p + s_p\Lambda_q q\right)^2 s k_\parallel \boldsymbol{q}_\Lambda^s(\boldsymbol{k})\,\boldsymbol{q}_{\Lambda_p}^{s_p}(\boldsymbol{p})\,\boldsymbol{q}_{\Lambda_q}^{s_q}(\boldsymbol{q}) \\ & \times \left[\frac{s k_\parallel}{\boldsymbol{q}_\Lambda^s(\boldsymbol{k})} - \frac{s_p p_\parallel}{\boldsymbol{q}_{\Lambda_p}^{s_p}(\boldsymbol{p})} - \frac{s_q q_\parallel}{\boldsymbol{q}_{\Lambda_q}^{s_q}(\boldsymbol{q})}\right] \delta(s k_\parallel - s_p p_\parallel - s_q q_\parallel)\,\delta_{k,pq}\,\mathrm{d}\boldsymbol{p}\,\mathrm{d}\boldsymbol{q}. \end{aligned} \tag{5.15}$$

This equation tells us that we only have a nonlinear contribution when the wave polarities s_p and s_q are different. We recover here a well-known property of incompressible MHD: the nonlinear interactions are only due to counterpropagating Alfvén waves. This remark leads eventually to the following simplified form:

$$\begin{aligned}\partial_t \boldsymbol{q}_\Lambda^s(\boldsymbol{k}) = {} & \frac{\pi\,\epsilon^2}{2\,b_0}\int \sum_{\Lambda_p,\Lambda_q} \left(\frac{\sin\psi_k}{k}\right)^2 (\Lambda k + \Lambda_p p + \Lambda_q q)^2 \left(\Lambda k - \Lambda_p p + \Lambda_q q\right)^2 \\ & \times \boldsymbol{q}_{\Lambda_p}^{-s}(\boldsymbol{p}) \left[\boldsymbol{q}_{\Lambda_q}^s(\boldsymbol{q}) - \boldsymbol{q}_\Lambda^s(\boldsymbol{k})\right] \delta(p_\parallel)\,\delta_{k,pq}\,\mathrm{d}\boldsymbol{p}\,\mathrm{d}\boldsymbol{q}. \end{aligned} \tag{5.16}$$

This result is exactly the same as in Galtier (2006*b*) (see in particular appendix D), where the MHD limit was discussed in the more general context of Hall MHD (the difference of a factor of 8 disappears after renormalization of the density tensor $\boldsymbol{q}_\Lambda^s(\boldsymbol{k})$). Note that the comparison with Galtier *et al.* (2000) is not direct since the complex helicity basis was not used. The presence of $\delta(p_\parallel)$ is due to the three-wave frequency resonance condition. This means that in any triadic resonant interaction, there is always one wave that corresponds to a purely two-dimensional motion ($p_\parallel = 0$), whereas the other two have equal parallel components ($p_\parallel = k_\parallel$). In other words, there is no nonlinear transfer along $\boldsymbol{b}_0$, and a cascade happens only in the perpendicular direction.

5.5. *Large-scale dynamics: inertial waves*

We consider the large-scale ($kd \rightarrow 0$) limit of (3.28) for left-handed ($\Lambda = -s$) fluctuations. Then, at leading order we have

$$\xi_\Lambda^s \rightarrow -\frac{skd}{2}, \tag{5.17}$$

$$\left(2 + (\xi_\Lambda^{-s})^2 (\xi_{\Lambda_p}^{-s_p})^2 (\xi_{\Lambda_q}^{-s_q})^2 - (\xi_\Lambda^{-s})^2 - (\xi_{\Lambda_p}^{-s_p})^2 - (\xi_{\Lambda_q}^{-s_q})^2\right)^2 \rightarrow \left(\frac{64}{k^2 p^2 q^2 d^6}\right)^2, \tag{5.18}$$

$$\omega_\Lambda^s \rightarrow \frac{2\Omega_0 s k_\parallel}{k} = \omega_I. \tag{5.19}$$

After substituting the preceding expressions into (3.28), we obtain

$$\begin{aligned} \partial_t \boldsymbol{q}_\Lambda^s(\boldsymbol{k}) &= \frac{\pi \epsilon^2}{4 b_0^2} \int \sum_{\Lambda_p, \Lambda_q} \left(\frac{\sin \psi_k}{k}\right)^2 (\Lambda k + \Lambda_p p + \Lambda_q q)^2 \frac{(\Lambda_q q - \Lambda_p p)^2}{p^2 q^2} \frac{k^2 \omega_\Lambda^{-\Lambda}}{k_\parallel^2} \\ &\quad \times \boldsymbol{q}_\Lambda^{-\Lambda}(\boldsymbol{k}) \boldsymbol{q}_{\Lambda_p}^{-\Lambda_p}(\boldsymbol{p}) \boldsymbol{q}_{\Lambda_q}^{-\Lambda_q}(\boldsymbol{q}) \left[\frac{k^2 \omega_\Lambda^{-\Lambda}}{\boldsymbol{q}_\Lambda^{-\Lambda}(\boldsymbol{k})} - \frac{p^2 \omega_{\Lambda_p}^{-\Lambda_p}}{\boldsymbol{q}_{\Lambda_p}^{-\Lambda_p}(\boldsymbol{p})} - \frac{q^2 \omega_{\Lambda_q}^{-\Lambda_q}}{\boldsymbol{q}_{\Lambda_q}^{-\Lambda_q}(\boldsymbol{q})}\right] \\ &\quad \times \delta(\Omega_{k,pq})\, \delta_{k,pq}\, \mathrm{d}\boldsymbol{p}\, \mathrm{d}\boldsymbol{q}. \end{aligned} \tag{5.20}$$

This result is exactly the same as in Galtier (2003), provided that the density tensor is correctly renormalized.

5.6. *Large-scale dynamics: magnetostrophic waves*

The last limit that we shall consider is the large-scale ($kd \rightarrow 0$) limit for right-handed ($\Lambda = s$) fluctuations. This limit is the most interesting one in the context of the magnetostrophic dynamo, because it describes the slow dynamics of the magnetic field which includes, as will be shown later, a direct and an inverse cascade. We have, at leading order,

$$\xi_\Lambda^s \rightarrow -\frac{2s}{kd}, \tag{5.21}$$

$$\left(2 + (\xi_\Lambda^{-s})^2 (\xi_{\Lambda_p}^{-s_p})^2 (\xi_{\Lambda_q}^{-s_q})^2 - (\xi_\Lambda^{-s})^2 - (\xi_{\Lambda_p}^{-s_p})^2 - (\xi_{\Lambda_q}^{-s_q})^2\right)^2 \rightarrow 4, \tag{5.22}$$

$$\omega_\Lambda^s \rightarrow \frac{s k_\parallel k d b_0}{2} = \omega_M. \tag{5.23}$$

After substituting the preceding expressions into (3.28), we obtain

$$\partial_t \boldsymbol{q}_\Lambda^s(\boldsymbol{k}) = \frac{\pi \epsilon^2}{b_0^2} \int \sum_{\Lambda_p, \Lambda_q} \left(\frac{\sin \psi_k}{k}\right)^2 (\Lambda k + \Lambda_p p + \Lambda_q q)^2 \left(\Lambda_p p - \Lambda_q q\right)^2 \frac{\omega_\Lambda^\Lambda}{k_\parallel^2}$$

$$\times\, \boldsymbol{q}_\Lambda^\Lambda(\boldsymbol{k})\boldsymbol{q}_{\Lambda_p}^{\Lambda_p}(\boldsymbol{p})\boldsymbol{q}_{\Lambda_q}^{\Lambda_q}(\boldsymbol{q}) \left[\frac{\omega_\Lambda^\Lambda}{\boldsymbol{q}_\Lambda^\Lambda(\boldsymbol{k})} - \frac{\omega_{\Lambda_p}^{\Lambda_p}}{\boldsymbol{q}_{\Lambda_p}^{\Lambda_p}(\boldsymbol{p})} - \frac{\omega_{\Lambda_q}^{\Lambda_q}}{\boldsymbol{q}_{\Lambda_q}^{\Lambda_q}(\boldsymbol{q})}\right]$$
$$\times\, \delta(\Omega_{k,pq})\,\delta_{k,pq}\,\mathrm{d}\boldsymbol{p}\,\mathrm{d}\boldsymbol{q}. \tag{5.24}$$

This system has never been analysed before; however, it is similar to the electron MHD case (Galtier & Bhattacharjee 2003). It is thought that this regime is relevant to describing solar wind turbulence at the sub-ion scale (Galtier 2009*b*); the observations and theoretical developments made in that context may also be useful in investigating the magnetostrophic regime, as they can be a source of inspiration. For example, it is interesting to mention that the existence of an inverse cascade of magnetic helicity in electron MHD has been proved numerically (Cho 2011).

6. Exact solutions for the turbulent spectra

We shall derive the exact solutions of the weak turbulence equations in three different limits: the large- and small-wavenumber limits, with in the latter case a distinction between right and left polarizations. To do so, we need to write the expression of the spectral density $\boldsymbol{q}_\Lambda^s(\boldsymbol{k})$ in terms of explicit quantities such as the kinetic and magnetic energies and the cross- and magnetic helicities. We invert the system $(E^u, E^b, H^c, H^m)(\boldsymbol{q}_\Lambda^s)$ and obtain

$$\boldsymbol{q}_\Lambda^s(\boldsymbol{k}) = \frac{1}{2[(\xi_\Lambda^s)^2 - (\xi_\Lambda^{-s})^2)]}$$
$$\times \left[(\xi_\Lambda^s)^2 E^b(\boldsymbol{k}) - E^u(\boldsymbol{k}) + (\xi_\Lambda^s + \xi_\Lambda^{-s})H^c(\boldsymbol{k}) + \Lambda\{(\xi_\Lambda^s)^2 - 1\}kH^m(\boldsymbol{k})\right]. \tag{6.1}$$

Substitution of expression (6.1) into (3.28) leads to weak turbulence equations for E^u, E^u, H^c and H^m. However, since we are only interested in the three asymptotic limits (of Alfvén, inertial and magnetostrophic wave turbulence) for which we are able to derive the solutions, we may simplify the problem by taking the asymptotic values of the coefficients ξ_Λ^s (see § 5). Note that for simplicity we will not consider interactions between left and right polarized waves in the large-scale ($kd \ll 1$) limit. We may suppose that these interactions are negligible anyway because of their different nonlinear time scales.

6.1. *Solutions for Alfvén wave turbulence*

The small-scale limit of Alfvén wave turbulence is very well known and has been analysed in detail by Galtier *et al.* (2000). For application to the dynamo it is not the most relevant limit, since the magnetic energy is expected to accumulate at the largest scales of the system. Therefore, we will not give details about this regime but only recall the main properties. In the small-scale limit ($kd \to +\infty$), for which terms like $(\xi_\Lambda^{-s})^2$ tend to 1, an equipartition between the kinetic and magnetic energies is obtained and their dynamical equations tend to be identical. If we neglect the helicity contributions, the equation for the total energy gets reduced (see the derivation given in Galtier (2006*b*), where the helicity decomposition is used), and it is then possible to demonstrate that the axisymmetric bi-dimensional total energy spectrum follows the universal solution

$$E(k_\perp, k_\parallel) \sim k_\perp^{-2} f(k_\parallel), \tag{6.2}$$

where f is an arbitrary function which traduces the dynamical decoupling of parallel planes in Fourier space. In other words, in Alfvén wave turbulence the cascade towards small scales happens only in the perpendicular direction. This regime with its predictions has been observed in direct numerical simulations (Bigot, Galtier & Politano 2008; Perez & Boldyrev 2008; Bigot & Galtier 2011).

6.2. *Solutions for inertial wave turbulence*

When the large-scale limit ($kd \to 0$) is taken with only the left polarization retained, one arrives at the inertial wave turbulence regime, which was derived analytically by Galtier (2003) and studied numerically by Bellet *et al.* (2006). Since $\xi_\Lambda^s \to 0$, we see immediately from relation (6.1) that the magnetic energy becomes negligible compared to the kinetic energy: in other words, the magnetic and kinetic energies with a left polarization are decoupled. Additionally, a simple analysis of (5.20) allows us to conclude that this turbulence becomes anisotropic. Indeed, if we assume that the nonlinear transfer is mainly the result of local interactions (in hydrodynamic turbulence, it is believed that the cascade mechanism is mainly due to local interactions: an eddy of a given size interacts mainly with eddies of slightly larger or smaller size; also, it is reasonable to start with the local interaction assumption in order to simplify the analysis, i.e. with equilateral triads $k \approx p \approx q$), then the resonance condition (3.26) simplifies to

$$\frac{s_p - s}{s s_p q_\parallel} \approx \frac{s_p - s_q}{s_p s_q k_\parallel} \approx \frac{s - s_q}{s s_q p_\parallel}. \tag{6.3}$$

From (5.20), we see that only the interactions between two waves ($\boldsymbol{p}$ and $\boldsymbol{q}$) with opposite polarities ($s = s_p = -s_q$ or $s = -s_p = s_q$, with $s = -\Lambda$) will contribute significantly to the nonlinear dynamics. This implies that either $q_\parallel \approx 0$ or $p_\parallel \approx 0$, which means that only a small transfer is allowed along $\boldsymbol{\Omega}_0$. In other words, the local nonlinear interactions lead to anisotropic turbulence, where small scales are preferentially generated perpendicularly to the external rotation axis. The anisotropy of the flow has been clearly observed experimentally in rotating hydrodynamics with different apparatus (Jacquin *et al.* 1990; Baroud *et al.* 2002; Morize *et al.* 2005; van Bokhoven *et al.* 2009). Note that this approximation is particularly well verified initially if the turbulence is mainly excited in a limited band of scales; then, by nature the nonlinear interactions will be local and will produce anisotropy. In the Earth's dynamo, with the forcing being due to convection, we would think that the range of excited scales is relatively limited (see figure 4). Then, this nonlinear mechanism of anisotropy production should operate. This short analysis allows us to consider the anisotropic limit of (5.20) for which $k_\perp \gg k_\parallel$. We obtain the following equations:

$$\begin{aligned}\frac{\partial}{\partial t}\begin{Bmatrix} E_k \\ H_k \end{Bmatrix} = \frac{\Omega^2\epsilon^2}{4} \sum_{s s_p s_q} \int \frac{s k_\parallel s_p p_\parallel}{k_\perp^2 p_\perp^2 q_\perp^2} \left(\frac{s_q q_\perp - s_p p_\perp}{\omega_k}\right)^2 (s k_\perp + s_p p_\perp + s_q q_\perp)^2 \sin\theta_q \\ \times \begin{Bmatrix} E_q(p_\perp E_k - k_\perp E_p) + (p_\perp s H_k/k_\perp - k_\perp s_p H_p/p_\perp) s_q H_q/q_\perp \\ s k_\perp [E_q(p_\perp s H_k/k_\perp - k_\perp s_p H_p/p_\perp) + (p_\perp E_k - k_\perp E_p) s_q H_q/q_\perp] \end{Bmatrix} \\ \times \delta(s\omega_k + s_p\omega_p + s_q\omega_q)\, \delta(k_\parallel + p_\parallel + q_\parallel)\, \mathrm{d}p_\perp\, \mathrm{d}q_\perp\, \mathrm{d}p_\parallel\, \mathrm{d}q_\parallel,\end{aligned} \tag{6.4}$$

where $E_k \equiv E^u(k_\perp, k_\parallel)$ and $H_k \equiv H^k(k_\perp, k_\parallel)$ are the axisymmetric bi-dimensional kinetic energy and kinetic helicity spectra, respectively, θ_q is the angle between the perpendicular wavevectors $\boldsymbol{k}_\perp$ and $\boldsymbol{p}_\perp$ in the triangle formed with ($\boldsymbol{k}_\perp$, $\boldsymbol{p}_\perp$, $\boldsymbol{q}_\perp$) and $\omega_k \simeq 2\Omega k_\parallel/k_\perp$. In (6.4), the integration over perpendicular wavenumbers is such that the triangular relation $\boldsymbol{k}_\perp + \boldsymbol{p}_\perp + \boldsymbol{q}_\perp = \boldsymbol{0}$ must be satisfied. The exact solutions of (6.4) were derived initially for a positive and constant kinetic energy flux (Galtier 2003); they read

$$E_k \sim k_\perp^{-5/2} |k_\parallel|^{-1/2}, \tag{6.5}$$

$$H_k \sim k_\perp^{-3/2} |k_\parallel|^{-1/2}. \tag{6.6}$$

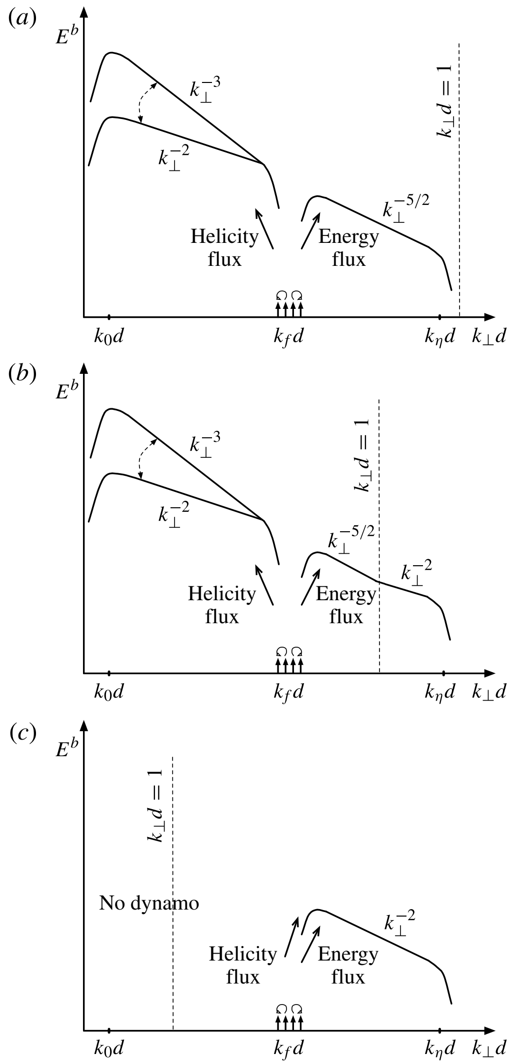

FIGURE 4. Magnetic energy spectrum with a (e.g. convective) forcing applied in a range of intermediate scales k_f, in (*a*) the pure magnetostrophic regime, (*b*) the magnetostrophic–Alfvén regime and (*c*) the pure Alfvén regime. In practice, the inertial ranges are limited by the largest scale of the system, k_0 (e.g. the size of the outer core), and the dissipative scale, k_η (e.g. the magnetic one). In (*a*), while the direct energy cascade gives a unique scaling, the inverse helicity cascade may lead to a family of solutions confined between $k_\perp^{-2}$ and $k_\perp^{-3}$, due to the entanglement of the helicity and energy. In (*b*), the same is expected, except for the smallest scales where we observe a transition from the magnetostrophic regime to the Alfvén regime with a change of slope. In the pure Alfvén regime of (*c*) we only have a direct cascade of energy and helicity, which does not allow a dynamo.

In a situation where the turbulence is dominated by a (forward) helicity flux, it is necessary to consider the equation for the kinetic helicity to derive the other exact power-law solutions. If we seek stationary solutions in the power-law form

$E_k \sim k_\perp^n |k_\parallel|^m$ and $H_k \sim k_\perp^{\tilde{n}} |k_\parallel|^{\tilde{m}}$, then the constant helicity flux solutions are more general and read (Galtier 2014)

$$n + \tilde{n} = -4, \tag{6.7}$$

$$m + \tilde{m} = -1. \tag{6.8}$$

These solutions correspond to a positive helicity flux and thus a direct cascade. The cascade along the rotation axis being strongly reduced, the most important scaling law is therefore the one for the perpendicular wavenumbers. It is remarkable to see that the exact solution (6.7) corresponds to the empirical law observed in many direct numerical simulations where the helicity transfer dominates the energy transfer (see e.g. Mininni & Pouquet 2009; Mininni *et al.* 2012). The domain of validity of this family of solutions is given by

$$-3 < n + m < -2, \tag{6.9}$$

$$-2 < \tilde{n} + \tilde{m} < -1. \tag{6.10}$$

The power-law indices are exact solutions of the weak turbulence equations only if the inequalities are satisfied: power-law spectra that do not satisfy the inequalities still describe weak turbulence in principle, but they cannot be produced by the system. The spectral solutions of the inertial wave turbulence regime are at the borderline of the domain of convergence. However, since the problem is strongly anisotropic and the inertial range in the parallel direction is strongly reduced with a cascade almost only in the perpendicular direction, we may neglect the inertial range in the parallel direction, which is equivalent to saying that $m = \tilde{m} = 0$. Then, we obtain a classical result of weak turbulence in the sense that the power-law indices of the exact solutions (6.5) and (6.6) fall exactly in the middle of the domains of locality, (6.9) and (6.10). In conclusion, we see that the turbulent spectra do not correspond necessarily to the so-called maximal helicity state, which is a particular solution of the Schwarz inequality $H(\boldsymbol{k}) \leqslant kE(\boldsymbol{k})$ (here we consider directly the weak turbulence limit for which the polarization term, as in Cambon & Jacquin 1989, does not contribute) and for which $n = \tilde{n} - 1 = -5/2$. As the helicity transfer increases, the power-law indices n and $\tilde{n}$ get closer. The condition of locality gives, however, a limit to this convergence, namely $n = \tilde{n} = -2$.

6.3. *Solutions for magnetostrophic wave turbulence*

The large-scale limit ($kd \to 0$) of expression (3.28) can lead to the magnetostrophic wave turbulence equations if only the right polarization is retained. Under this limit, the kinetic energy becomes negligible compared to the magnetic energy; in other words, the magnetic and kinetic energies with a right polarization are decoupled. As for inertial wave turbulence, we may show from (5.20) that this turbulence becomes naturally anisotropic. Indeed, if we consider that the nonlinear transfer is mainly due to local interactions ($k \approx p \approx q$), the resonance condition (3.26) simplifies to

$$\frac{s_p - s}{q_\parallel} \approx \frac{s_p - s_q}{k_\parallel} \approx \frac{s - s_q}{p_\parallel}. \tag{6.11}$$

From (5.24), we see that only the interactions between two waves $\boldsymbol{p}$ and $\boldsymbol{q}$ with opposite polarities ($s = s_p = -s_q$ or $s = -s_p = s_q$, with $s = \Lambda$) will contribute significantly to the nonlinear dynamics. This implies that either $q_\parallel \approx 0$ or $p_\parallel \approx 0$, which means that only a small transfer is allowed along $\boldsymbol{\Omega}_0$. As for inertial wave turbulence, (i) the local nonlinear interactions lead to anisotropic turbulence where the cascade is preferentially generated perpendicularly to the external rotation axis, and (ii) the approximation is particularly well verified initially if the turbulence is mainly excited in a limited band of scales, as then by nature the nonlinear interactions will be local. From this discussion, it seems relevant to take the anisotropic limit ($k_\perp \gg k_\parallel$) of (5.24), which gives

$$\partial_t \begin{Bmatrix} E_k \\ H_k \end{Bmatrix} = \frac{\epsilon^2 d}{8b_0} \sum_{ss_ps_q} \int \frac{s_p p_\perp k_\parallel p_\parallel}{q_\perp} \left(\frac{s_q q_\perp - s_p p_\perp}{k_\parallel}\right)^2 (sk_\perp + s_p p_\perp + s_q q_\perp)^2 \sin\theta_q \\ \times \begin{Bmatrix} sk_\perp [E_q(p_\perp E_k - k_\perp E_p)/(k_\perp p_\perp q_\perp) + s_q H_q (sH_k - s_p H_p)] \\ E_q(sH_k - s_p H_p)/q_\perp + s_q H_q (p_\perp E_k - k_\perp E_p)/(k_\perp p_\perp) \end{Bmatrix} \\ \times \delta(k_\parallel + p_\parallel + q_\parallel)\, \delta(sk_\perp k_\parallel + s_p p_\perp p_\parallel + s_q q_\perp q_\parallel)\, \mathrm{d}p_\perp\, \mathrm{d}q_\perp\, \mathrm{d}p_\parallel\, \mathrm{d}q_\parallel, \quad (6.12)$$

where $E_k \equiv E^b(k_\perp, k_\parallel)$ and $H_k \equiv H^m(k_\perp, k_\parallel)$ are the axisymmetric bi-dimensional magnetic energy and magnetic helicity spectra, respectively, and as before θ_q is the angle between the perpendicular wavevectors $\boldsymbol{k}_\perp$ and $\boldsymbol{p}_\perp$ in the triangle formed by $(\boldsymbol{k}_\perp, \boldsymbol{p}_\perp, \boldsymbol{q}_\perp)$. In (6.12), the integration over perpendicular wavenumbers is such that the triangular relation $\boldsymbol{k}_\perp + \boldsymbol{p}_\perp + \boldsymbol{q}_\perp = \boldsymbol{0}$ must be satisfied. To derive the exact solutions, we have to introduce the following power-law forms for the spectra $E_k \sim k_\perp^n |k_\parallel|^m$ and $H_k \sim k_\perp^{\tilde{n}} |k_\parallel|^{\tilde{m}}$, and apply a bi-homogeneous conformal transform (Kuznetsov 1972; Zakharov *et al.* 1992; Nazarenko 2011) which involves performing the following manipulation on the wavenumbers $p_\perp$, $q_\perp$, $p_\parallel$ and $q_\parallel$:

$$\left.\begin{aligned} p_\perp &\rightarrow k_\perp^2/p_\perp, \\ q_\perp &\rightarrow k_\perp q_\perp/p_\perp, \\ |p_\parallel| &\rightarrow k_\parallel^2/|p_\parallel|, \\ |q_\parallel| &\rightarrow |k_\parallel||q_\parallel|/|p_\parallel|. \end{aligned}\right\} \quad (6.13)$$

This exercise for the energy equation gives the positive and constant energy flux solutions

$$E_k \sim k_\perp^{-5/2} |k_\parallel|^{-1/2}, \quad (6.14)$$
$$H_k \sim k_\perp^{-7/2} |k_\parallel|^{-1/2}. \quad (6.15)$$

The same transform applied to the helicity equation extends the preceding solutions to a family of solutions (a detailed derivation is given in appendix D)

$$n + \tilde{n} = -6, \quad (6.16)$$
$$m + \tilde{m} = -1. \quad (6.17)$$

This family of solutions corresponds to a negative and constant magnetic helicity flux, hence implying the possible existence of an inverse cascade of helicity and the accumulation of magnetic energy at large scales (see appendix E for a rigorous demonstration). Since the cascade along the uniform magnetic field is strongly reduced, the most important scaling law is therefore the one for the perpendicular wavenumbers. The domain of validity of these solutions can be written as

$$-3 < n + m < -2, \quad (6.18)$$
$$-4 < \tilde{n} + \tilde{m} < -3. \quad (6.19)$$

We see that with the previous solutions (obtained from the energy or the helicity equations) we are at the borderline of the domain of convergence. However, we also know that this problem is strongly anisotropic and the inertial range in the parallel direction is strongly reduced with a cascade almost only in the perpendicular direction. Actually, if we neglect the inertial range in the parallel direction (which is equivalent to taking $m = \tilde{m} = 0$) we again obtain – as for the inertial wave turbulence regime – a classical result of weak turbulence in the sense that the power-law indices of the exact solutions (6.14) and (6.15) fall exactly in the middle of the domains of locality (6.18) and (6.19). Note that the solutions found do not allow a crossing of the spectra, since the case $n = \tilde{n} = -3$ appears as an asymptotic limit. Note also that the classical phenomenology presented in § 4 gives the particular asymptotic solution $\tilde{n} = -3$. It is only through a deep mathematical treatment that this family of solutions may be discovered. This situation is also found for the inertial wave turbulence regime, to which many papers have been devoted but where no consistent anisotropic phenomenology has been proposed. For that reason, these exact solutions may be considered highly non-trivial. Finally, it is interesting to note that the process of inverse cascade described here is limited in scale, since the basic assumption made for the analysis is that $k_\perp \gg k_\parallel$. When this condition is violated (with $k_\perp \ll k_\parallel$, for example), the previous local analysis done on the resonance condition becomes irrelevant and the theoretical predictions are not possible.

7. Discussion

In this paper a weak turbulence theory has been developed for rotating MHD in the presence of a parallel uniform magnetic field. The theory is expected to be relevant for the magnetostrophic dynamo, with applications to the Earth and to giant planets for which a small ($\sim 10^{-6}$) Rossby number is expected. An important question investigated here is the mechanism of regeneration of a large-scale magnetic field through an inverse cascade of hybrid helicity. A key length scale in this problem is the magneto-inertial length d, which indicates the basin of attraction for the dynamics. Basically, if the scales considered are larger than d (in other words, if $kd < 1$), we fall in the inertial or magnetostrophic wave turbulence regime, the precise localization being determined by the nature of the polarization (left or right, respectively). If, however, the scales are smaller than d ($kd > 1$) and the conditions for weak turbulence are still satisfied (with a wave period much smaller than the eddy-turnover time; otherwise the turbulence is strong), then we fall in the Alfvén wave turbulence regime. It is interesting to note that the magnetostrophic regime – also called the strong-field regime – is driven by the nonlinear equation (2.28), similar to a well-known system in plasma physics called electron MHD (Kingsep *et al.* 1990), which finds applications in space plasmas (Galtier 2006*a*), for example. We have checked that a derivation of the weak turbulence equations made directly from expression (2.28) also gives (5.24). Thus, the magnetostrophic regime characterized by a balance between the Coriolis and Lorentz–Laplace forces can be described simply by (2.28) instead of the system comprising (2.1) and (2.2).

By using a complex helicity decomposition, the asymptotic weak turbulence equations have been derived which describe the long-time behaviour of weakly dispersive interacting waves via three-wave processes. For magnetostrophic wave turbulence, the theory predicts that the magnetic energy is asymptotically larger than the kinetic energy when one goes to large scales, whereas the reverse holds for inertial wave turbulence. Analysis of the resonance conditions has been used to prove the anisotropic nature of the nonlinear transfer, with a stronger cascade perpendicular than parallel to the rotation axis. Then, the reduced forms of the general equations of weak turbulence were obtained in the three relevant limits discussed above, along with their exact power-law solutions, after application of the Kuznetsov–Zakharov transform (see figure 4). The large-scale (magnetostrophic and inertial) solutions can be highly non-trivial (i.e. impossible to find intuitively) in the sense that the classical phenomenology of weak turbulence that we introduced in § 4 is only able to predict the correct scaling for the constant energy flux solutions. The solutions for the constant (magnetic or kinetic) helicity flux are, however, not recovered with the phenomenology. The non-trivial solutions implying the energy and helicity spectra power-law indices can be found only after a long and rigorous derivation.

At large scales ($kd < 1$), whereas a direct cascade of kinetic helicity is expected which is well observed in direct numerical simulations of pure rotating hydrodynamic turbulence (see e.g. Mininni & Pouquet 2009; Mininni *et al.* 2012), an inverse cascade of magnetic helicity is predicted. Since the magnetostrophic wave turbulence regime is similar to the electron MHD one, where an inverse cascade has already been observed in direct numerical simulations (Shaikh & Zank 2005; Cho 2011), we think that it is a reasonable prediction. Then, in the context of the dynamo problem, the main question is: at which scale k_f is the system driven? Indeed, if the forcing scale is such that $k_f d < 1$, we fall in the large-scale regime (magnetostrophic basin of attraction; see figure 4), and the dynamo mechanism may happen through an inverse cascade of hybrid helicity which is dominated by the magnetic helicity. However, if the scale is such that $k_f d > 1$, then we fall in the small-scale regime (Alfvén basin of attraction), and the regeneration of the magnetic field becomes more difficult since the hybrid helicity is dominated by the cross-helicity which cascades in the forward (to small scales) direction (Galtier *et al.* 2000). It is important to recall that the magnetic helicity is not an inviscid invariant in the weak (non-rotating) MHD turbulence regime where a uniform magnetic field is present; in our framework, the question of the regeneration of a large-scale magnetic field therefore needs a new ingredient such as the Coriolis force to be relevant.

The present theory may be useful in gaining a better understanding of the magnetostrophic dynamo, with applications to the Earth and giant planets. Although our theory is a crude model for such a problem (for instance, we assume a magnetic Reynolds number large enough for the development of an extended inertial range and do not include the geometry effects with boundary conditions), it is believed that the dynamics obtained here at asymptotically small Rossby numbers opens up new perspectives. For example, in the case of the outer core of the Earth, a rough evaluation of the magneto-inertial length gives $d \approx 1$ km (Finlay *et al.* 2010). If we consider that the forcing due to convection has a typical length scale of $1/k_f \approx 100$ km, then the conditions for an inverse cascade are satisfied. Another question concerns the surprising axisymmetry of planets like Earth, Jupiter or Saturn, where the rotation and magnetic axes are close – even almost perfect for Saturn. The present turbulence theory gives a possible (although speculative) answer. Indeed, the rotating MHD equations in the presence of a uniform magnetic field have in general only one inviscid invariant, namely the total energy. It is only when the rotation and magnetic axes are aligned that a second inviscid invariant appears, namely the hybrid helicity. It is precisely this second invariant which can generate a turbulent dynamo through an inverse cascade. We believe that as long as the angle θ between $\boldsymbol{\Omega}_0$ and $\boldsymbol{b}_0$ remains reasonably small, the inverse cascade can still operate. According to this remark, it is not surprising that a strong alignment, with $\theta \leqslant 10°$, is generally observed for the aforementioned magnetized planets. The initial phase of the dynamo has not been discussed so far, but it deserves a brief mention. Since in the absence of a uniform magnetic field the magnetic helicity is an inviscid invariant of rotating MHD, an inverse cascade may happen. This mechanism is, however, under the influence of the Coriolis force, which renders the dynamics anisotropic. We may then expect the generation of a large-scale magnetic field preferentially aligned with the rotation axis. After this initial phase, it seems natural to consider the regime described in the present paper. By extension, it may even be that the present analysis is relevant for exoplanets and some magnetized stars (Morin *et al.* 2011).

Appendix A. Useful relationships

From the quantity

$$\xi_\Lambda^s = \frac{-skd}{-s\Lambda + \sqrt{1+k^2d^2}} \tag{A 1}$$

it is possible to derive the following useful identities:

$$\xi_\Lambda^s \xi_\Lambda^{-s} = -1, \tag{A 2}$$

$$\xi_{-\Lambda}^{-s} = -\xi_\Lambda^s, \tag{A 3}$$

$$\xi_\Lambda^s + \xi_\Lambda^{-s} = -\frac{2}{\Lambda kd}, \tag{A 4}$$

$$\xi_\Lambda^s - \xi_\Lambda^{-s} = -\frac{2s}{kd}\sqrt{1+k^2d^2}, \tag{A 5}$$

$$1 - (\xi_\Lambda^s)^2 = \frac{2\Lambda\Omega_0}{b_0 k}\,\xi_\Lambda^s. \tag{A 6}$$

We also have the remarkable relations

$$\omega_s^s \omega_{-s}^s = (k_\parallel \boldsymbol{b}_0)^2, \tag{A 7}$$

$$(\omega_s^s)^2 \leqslant (k_\parallel \boldsymbol{b}_0)^2 \leqslant (\omega_{-s}^s)^2. \tag{A 8}$$

Appendix B. Helicity decomposition

Projection of the Fourier transform of the original vectors $\boldsymbol{u}(\boldsymbol{x})$ and $\boldsymbol{b}(\boldsymbol{x})$ onto the helicity basis gives

$$\boldsymbol{u}_{\boldsymbol{k}} = \sum_\Lambda \mathscr{U}_\Lambda(\boldsymbol{k})\,\boldsymbol{h}_{\boldsymbol{k}}^{\Lambda}, \tag{B 1}$$

$$\boldsymbol{b}_{\boldsymbol{k}} = \sum_\Lambda \mathscr{B}_\Lambda(\boldsymbol{k})\,\boldsymbol{h}_{\boldsymbol{k}}^{\Lambda}. \tag{B 2}$$

If we invert the system, we find the following relations for the velocity components:

$$\mathscr{U}_+(\boldsymbol{k}) = \frac{1}{2kk_\perp}\left[k_x k_\parallel u_x + k_y k_\parallel u_y - k_\perp^2 u_z + \mathrm{i}k(k_y u_x - k_x u_y)\right], \tag{B 3}$$

$$\mathscr{U}_-(\boldsymbol{k}) = \frac{1}{2kk_\perp}\left[k_x k_\parallel u_x + k_y k_\parallel u_y - k_\perp^2 u_z - \mathrm{i}k(k_y u_x - k_x u_y)\right]. \tag{B 4}$$

Similar relations are found for the magnetic field. Note that such a helicity decomposition cannot be used for the modes $k_\perp = 0$.

Appendix C. Derivation of the weak turbulence equations

The starting point of the derivation of the weak turbulence equations is the fundamental equation (3.19). We write successively equations for the second- and third-order moments,

$$\partial_t \langle a^s_\Lambda a^{s'}_{\Lambda'} \rangle = \frac{\epsilon\, d^2}{16} \int \sum_{\substack{\Lambda_p,\Lambda_q \\ s_p,s_q}} \frac{\xi^{-s_q}_{\Lambda_q} - \xi^{-s_p}_{\Lambda_p}}{\xi^s_\Lambda - \xi^{-s}_\Lambda} \boldsymbol{M}^{\Lambda\Lambda_p\Lambda_q}_{\substack{s\, s_p\, s_q \\ -k\, p\, q}} \langle a^{s_p}_{\Lambda_p} a^{s_q}_{\Lambda_q} a^{s'}_{\Lambda'} \rangle\, \mathrm{e}^{-\mathrm{i}\Omega_{pq,k}t}\, \delta_{pq,k}\, \mathrm{d}\boldsymbol{p}\, \mathrm{d}\boldsymbol{q} + \frac{\epsilon\, d^2}{16} \int \sum_{\substack{\Lambda_p,\Lambda_q \\ s_p,s_q}} \frac{\xi^{-s_q}_{\Lambda_q} - \xi^{-s_p}_{\Lambda_p}}{\xi^{s'}_{\Lambda'} - \xi^{-s'}_{\Lambda'}} \boldsymbol{M}^{\Lambda'\Lambda_p\Lambda_q}_{\substack{s'\, s_p\, s_q \\ -k'\, p\, q}} \langle a^{s_p}_{\Lambda_p} a^{s_q}_{\Lambda_q} a^{s}_{\Lambda} \rangle \mathrm{e}^{-\mathrm{i}\Omega_{pq,k'}t}\, \delta_{pq,k'}\, \mathrm{d}\boldsymbol{p}\, \mathrm{d}\boldsymbol{q} \tag{C 1}$$

and

$$\partial_t \langle a^s_\Lambda a^{s'}_{\Lambda'} a^{s''}_{\Lambda''} \rangle = \frac{\epsilon\, d^2}{16} \int \sum_{\substack{\Lambda_p,\Lambda_q \\ s_p,s_q}} \frac{\xi^{-s_q}_{\Lambda_q} - \xi^{-s_p}_{\Lambda_p}}{\xi^s_\Lambda - \xi^{-s}_\Lambda} \boldsymbol{M}^{\Lambda\Lambda_p\Lambda_q}_{\substack{s\, s_p\, s_q \\ -k\, p\, q}} \langle a^{s_p}_{\Lambda_p} a^{s_q}_{\Lambda_q} a^{s'}_{\Lambda'} a^{s''}_{\Lambda''} \rangle \times \mathrm{e}^{-\mathrm{i}\Omega_{pq,k}t}\, \delta_{pq,k}\, \mathrm{d}\boldsymbol{p}\, \mathrm{d}\boldsymbol{q} + \frac{\epsilon\, d^2}{16} \int \sum_{\substack{\Lambda_p,\Lambda_q \\ s_p,s_q}} \frac{\xi^{-s_q}_{\Lambda_q} - \xi^{-s_p}_{\Lambda_p}}{\xi^{s'}_{\Lambda'} - \xi^{-s'}_{\Lambda'}} \times \boldsymbol{M}^{\Lambda'\Lambda_p\Lambda_q}_{\substack{s'\, s_p\, s_q \\ -k'\, p\, q}} \langle a^{s_p}_{\Lambda_p} a^{s_q}_{\Lambda_q} a^{s}_{\Lambda} a^{s''}_{\Lambda''} \rangle \mathrm{e}^{-\mathrm{i}\Omega_{pq,k'}t}\, \delta_{pq,k'}\, \mathrm{d}\boldsymbol{p}\, \mathrm{d}\boldsymbol{q} + \frac{\epsilon\, d^2}{16} \int \sum_{\substack{\Lambda_p,\Lambda_q \\ s_p,s_q}} \frac{\xi^{-s_q}_{\Lambda_q} - \xi^{-s_p}_{\Lambda_p}}{\xi^{s''}_{\Lambda''} - \xi^{-s''}_{\Lambda''}} \boldsymbol{M}^{\Lambda''\Lambda_p\Lambda_q}_{\substack{s''\, s_p\, s_q \\ -k''\, p\, q}} \langle a^{s_p}_{\Lambda_p} a^{s_q}_{\Lambda_q} a^{s}_{\Lambda} a^{s'}_{\Lambda'} \rangle \times \mathrm{e}^{-\mathrm{i}\Omega_{pq,k''}t}\, \delta_{pq,k''}\, \mathrm{d}\boldsymbol{p}\, \mathrm{d}\boldsymbol{q}. \tag{C 2}$$

We shall write an asymptotic closure (Nazarenko 2011) for our system. For that, we basically need to write the fourth-order moment in terms of a sum of the fourth-order cumulant and products of second-order ones. The asymptotic closure depends on two ingredients: one is the degree to which the linear waves interact to randomize phases, and the other relies on the fact that the nonlinear regeneration of the third-order moment by the fourth-order moment in (C 2) depends more on the product of the second-order moments than it does on the fourth-order cumulant. The fourth-order moment decomposes into the sum of three products of second-order moments and a fourth-order cumulant. The latter does not contribute to secular behaviour, and of the other products one is absent because of the homogeneity assumption. If we use the symmetric relations (3.21)–(3.24) and perform wavevector integrations, summations over polarities and time integration, then (C 2) becomes

$$\langle a^s_\Lambda a^{s'}_{\Lambda'} a^{s''}_{\Lambda''} \rangle = \frac{\epsilon\, d^2}{16} \Delta(\Omega_{kk'k''})\, \delta_{kk'k''} \times \left\{ \left[\frac{\xi^{-s''}_{\Lambda''} - \xi^{-s'}_{\Lambda'}}{\xi^s_\Lambda - \xi^{-s}_\Lambda} \left(\boldsymbol{M}^{\Lambda\Lambda'\Lambda''}_{\substack{s\, s'\, s'' \\ k\, k'\, k''}} \right)^* + \frac{\xi^{-s'}_{\Lambda'} - \xi^{-s''}_{\Lambda''}}{\xi^s_\Lambda - \xi^{-s}_\Lambda} \left(\boldsymbol{M}^{\Lambda\Lambda''\Lambda'}_{\substack{s\, s''\, s' \\ k\, k''\, k'}} \right)^* \right] \boldsymbol{q}^{s'}_{\Lambda'}\, \boldsymbol{q}^{s''}_{\Lambda''} \right.$$

$$+\left[\frac{\xi_{\Lambda''}^{-s''}-\xi_{\Lambda}^{-s}}{\xi_{\Lambda'}^{s'}-\xi_{\Lambda'}^{-s'}}\begin{pmatrix}\boldsymbol{M}\,{}^{\Lambda'\Lambda\Lambda''}_{s'ss''}\\ k'\,k\,k''\end{pmatrix}^{*}+\frac{\xi_{\Lambda}^{-s}-\xi_{\Lambda''}^{-s''}}{\xi_{\Lambda'}^{s'}-\xi_{\Lambda'}^{-s'}}\begin{pmatrix}\boldsymbol{M}\,{}^{\Lambda'\Lambda''\Lambda}_{s's''s}\\ k'\,k''\,k\end{pmatrix}^{*}\right]\boldsymbol{q}_{\Lambda}^{s}\,\boldsymbol{q}_{\Lambda''}^{s''}$$
$$+\left[\frac{\xi_{\Lambda}^{-s}-\xi_{\Lambda'}^{-s'}}{\xi_{\Lambda''}^{s''}-\xi_{\Lambda''}^{-s''}}\begin{pmatrix}\boldsymbol{M}\,{}^{\Lambda''\Lambda'\Lambda}_{s''s's}\\ k''\,k'\,k\end{pmatrix}^{*}+\frac{\xi_{\Lambda'}^{-s'}-\xi_{\Lambda}^{-s}}{\xi_{\Lambda''}^{s''}-\xi_{\Lambda''}^{-s''}}\begin{pmatrix}\boldsymbol{M}\,{}^{\Lambda''\Lambda\Lambda'}_{s''ss'}\\ k''\,k\,k'\end{pmatrix}^{*}\right]\boldsymbol{q}_{\Lambda'}^{s'}\,\boldsymbol{q}_{\Lambda}^{s}\Bigg\},\tag{C 3}$$

where

$$\Delta(\Omega_{kk'k''})=\int_0^t \mathrm{e}^{\mathrm{i}\Omega_{kk'k''}t'}\,\mathrm{d}t'=\frac{\mathrm{e}^{\mathrm{i}\Omega_{kk'k''}t}-1}{\mathrm{i}\Omega_{kk'k''}}.\tag{C 4}$$

Plugging the symmetric relations (3.21)–(3.24) into (C 3) allows us to simplify the previous equation further; one obtains

$$\begin{aligned}\langle a_{\Lambda}^{s}a_{\Lambda'}^{s'}a_{\Lambda''}^{s''}\rangle &= \frac{\epsilon\,d^2}{8}\,\Delta(\Omega_{kk'k''})\,\delta_{kk'k''}\begin{pmatrix}\boldsymbol{M}\,{}^{\Lambda\Lambda'\Lambda''}_{ss's''}\\ k\,k'\,k''\end{pmatrix}^{*}\\ &\times\left[\frac{\xi_{\Lambda''}^{-s''}-\xi_{\Lambda'}^{-s'}}{\xi_{\Lambda}^{s}-\xi_{\Lambda}^{-s}}\boldsymbol{q}_{\Lambda'}^{s'}\,\boldsymbol{q}_{\Lambda''}^{s''}+\frac{\xi_{\Lambda}^{-s}-\xi_{\Lambda''}^{-s''}}{\xi_{\Lambda'}^{s'}-\xi_{\Lambda'}^{-s'}}\boldsymbol{q}_{\Lambda}^{s}\,\boldsymbol{q}_{\Lambda''}^{s''}+\frac{\xi_{\Lambda'}^{-s'}-\xi_{\Lambda}^{-s}}{\xi_{\Lambda''}^{s''}-\xi_{\Lambda''}^{-s''}}\boldsymbol{q}_{\Lambda}^{s}\,\boldsymbol{q}_{\Lambda'}^{s'}\right].\end{aligned}\tag{C 5}$$

We substitute expression (C 5) into (C 1); this leads to

$$\begin{aligned}\partial_t\boldsymbol{q}_{\Lambda}^{s}(\boldsymbol{k}) &= \frac{\epsilon^2 d^4}{128}\int\sum_{\substack{\Lambda_p,\Lambda_q\\ s_p,s_q}}\frac{\xi_{\Lambda_q}^{-s_q}-\xi_{\Lambda_p}^{-s_p}}{\xi_{\Lambda}^{s}-\xi_{\Lambda}^{-s}}\left|\begin{matrix}\boldsymbol{M}\,{}^{\Lambda\Lambda_p\Lambda_q}_{s\,s_p\,s_q}\\ -k\,p\,q\end{matrix}\right|^2\Delta(\Omega_{pq,k})\,\mathrm{e}^{-\mathrm{i}\Omega_{pq,k}t}\,\delta_{pq,k}\\ &\times\left[\frac{\xi_{\Lambda}^{-s}-\xi_{\Lambda_q}^{-s_q}}{\xi_{\Lambda_p}^{s_p}-\xi_{\Lambda_p}^{-s_p}}\boldsymbol{q}_{\Lambda}^{s}\,\boldsymbol{q}_{\Lambda_q}^{s_q}+\frac{\xi_{\Lambda_p}^{-s_p}-\xi_{\Lambda}^{-s}}{\xi_{\Lambda_q}^{s_q}-\xi_{\Lambda_q}^{-s_q}}\boldsymbol{q}_{\Lambda}^{s}\,\boldsymbol{q}_{\Lambda_p}^{s_p}+\frac{\xi_{\Lambda_q}^{-s_q}-\xi_{\Lambda_p}^{-s_p}}{\xi_{\Lambda}^{s}-\xi_{\Lambda}^{-s}}\boldsymbol{q}_{\Lambda_p}^{s_p}\,\boldsymbol{q}_{\Lambda_q}^{s_q}\right]\mathrm{d}\boldsymbol{p}\,\mathrm{d}\boldsymbol{q}\\ &+\frac{\epsilon^2 d^4}{128}\int\sum_{\substack{\Lambda_p,\Lambda_q\\ s_p,s_q}}\frac{\xi_{\Lambda_q}^{-s_q}-\xi_{\Lambda_p}^{-s_p}}{\xi_{\Lambda'}^{s'}-\xi_{\Lambda'}^{-s'}}\left|\begin{matrix}\boldsymbol{M}\,{}^{\Lambda'\Lambda_p\Lambda_q}_{s'\,s_p\,s_q}\\ -k'\,p\,q\end{matrix}\right|^2\Delta(\Omega_{pq,k'})\,\mathrm{e}^{-\mathrm{i}\Omega_{pq,k'}t}\,\delta_{pq,k'}\\ &\times\left[\frac{\xi_{\Lambda'}^{-s'}-\xi_{\Lambda_q}^{-s_q}}{\xi_{\Lambda_p}^{s_p}-\xi_{\Lambda_p}^{-s_p}}\boldsymbol{q}_{\Lambda'}^{s'}\,\boldsymbol{q}_{\Lambda_q}^{s_q}+\frac{\xi_{\Lambda_p}^{-s_p}-\xi_{\Lambda'}^{-s'}}{\xi_{\Lambda_q}^{s_q}-\xi_{\Lambda_q}^{-s_q}}\boldsymbol{q}_{\Lambda'}^{s'}\,\boldsymbol{q}_{\Lambda_p}^{s_p}\right.\\ &\left.+\frac{\xi_{\Lambda_q}^{-s_q}-\xi_{\Lambda_p}^{-s_p}}{\xi_{\Lambda'}^{s'}-\xi_{\Lambda'}^{-s'}}\boldsymbol{q}_{\Lambda_p}^{s_p}\,\boldsymbol{q}_{\Lambda_q}^{s_q}\right]\mathrm{d}\boldsymbol{p}\,\mathrm{d}\boldsymbol{q}.\end{aligned}\tag{C 6}$$

The long-time behaviour of the weak turbulence equation (C 6) is given by the Riemman–Lebesgue lemma, which tells us that for $t\rightarrow+\infty$,

$$\mathrm{e}^{-\mathrm{i}xt}\Delta(x)=\Delta(-x)\rightarrow\pi\delta(x)-\mathrm{i}\mathscr{P}(1/x),\tag{C 7}$$

where $\mathscr{P}$ is the principal value of the integral. The two terms of (C 6) are complex-conjugates, so if in the second term we replace the dummy integration variables $\boldsymbol{p}$

and $\boldsymbol{q}$ by $-\boldsymbol{p}$ and $-\boldsymbol{q}$, we can simplify (C 6) further since, in particular, principal value terms compensate each other exactly. Finally, we obtain the weak turbulence equation

$$\begin{aligned}\partial_t \boldsymbol{q}_\Lambda^s(\boldsymbol{k}) &= \frac{\pi\,\epsilon^2 d^4}{64}\int \sum_{\substack{\Lambda_p,\Lambda_q\\ s_p,s_q}} \frac{\xi_{\Lambda_q}^{-s_q}-\xi_{\Lambda_p}^{-s_p}}{\xi_\Lambda^s-\xi_\Lambda^{-s}} \left| \boldsymbol{M}\,{}^{\Lambda\Lambda_p\Lambda_q}_{\substack{s\,s_p\,s_q\\ -k\,p\,q}} \right|^2 \delta(\Omega_{k,pq})\,\delta_{k,pq} \\ &\times \left[\frac{\xi_\Lambda^{-s}-\xi_{\Lambda_q}^{-s_q}}{\xi_{\Lambda_p}^{s_p}-\xi_{\Lambda_p}^{-s_p}}\,\boldsymbol{q}_\Lambda^s\,\boldsymbol{q}_{\Lambda_q}^{s_q} + \frac{\xi_{\Lambda_p}^{-s_p}-\xi_\Lambda^{-s}}{\xi_{\Lambda_q}^{s_q}-\xi_{\Lambda_q}^{-s_q}}\,\boldsymbol{q}_\Lambda^s\,\boldsymbol{q}_{\Lambda_p}^{s_p} \right. \\ &\left. + \frac{\xi_{\Lambda_q}^{-s_q}-\xi_{\Lambda_p}^{-s_p}}{\xi_\Lambda^s-\xi_\Lambda^{-s}}\,\boldsymbol{q}_{\Lambda_p}^{s_p}\,\boldsymbol{q}_{\Lambda_q}^{s_q}\right] \mathrm{d}\boldsymbol{p}\,\mathrm{d}\boldsymbol{q}, \end{aligned} \tag{C 8}$$

where

$$\begin{aligned}\left| \boldsymbol{M}\,{}^{\Lambda\Lambda_p\Lambda_q}_{\substack{s\,s_p\,s_q\\ -k\,p\,q}} \right|^2 &= \left(\frac{\sin\psi_k}{k}\right)^2 k^2p^2q^2\,(\Lambda k+\Lambda_p p+\Lambda_q q)^2(\xi_\Lambda^s)^2(\xi_{\Lambda_p}^{s_p})^2(\xi_{\Lambda_q}^{s_q})^2 \\ &\times \left(2+(\xi_\Lambda^{-s})^2(\xi_{\Lambda_p}^{-s_p})^2(\xi_{\Lambda_q}^{-s_q})^2-(\xi_\Lambda^{-s})^2-(\xi_{\Lambda_p}^{-s_p})^2-(\xi_{\Lambda_q}^{-s_q})^2\right)^2. \end{aligned} \tag{C 9}$$

The last step that we have to take to obtain the same expression as (3.28) is to include the resonance relations (3.26) in the previous equations. Additionally, since the dissipative terms are linear, one can easily add their contributions to the weak turbulence equations. Then, we obtain

$$\begin{aligned}&\partial_t \boldsymbol{q}_\Lambda^s(\boldsymbol{k}) \\ &= -2\kappa k^2 \boldsymbol{q}_\Lambda^s(\boldsymbol{k}) + \frac{\pi\,\epsilon^2 d^4}{64\,b_0^2}\int\sum_{\substack{\Lambda_p,\Lambda_q\\ s_p,s_q}} \left(\frac{\sin\psi_k}{k}\right)^2 k^2p^2q^2(\Lambda k+\Lambda_p p+\Lambda_q q)^2(\xi_\Lambda^s)^2(\xi_{\Lambda_p}^{s_p})^2(\xi_{\Lambda_q}^{s_q})^2 \\ &\times \left(\frac{\xi_{\Lambda_q}^{-s_q}-\xi_{\Lambda_p}^{-s_p}}{k_\parallel}\right)^2 \left(2+(\xi_\Lambda^{-s})^2(\xi_{\Lambda_p}^{-s_p})^2(\xi_{\Lambda_q}^{-s_q})^2-(\xi_\Lambda^{-s})^2-(\xi_{\Lambda_p}^{-s_p})^2-(\xi_{\Lambda_q}^{-s_q})^2\right)^2 \\ &\times \left(\frac{\omega_\Lambda^s}{1+(\xi_\Lambda^{-s})^2}\right) \boldsymbol{q}_\Lambda^s(\boldsymbol{k})\,\boldsymbol{q}_{\Lambda_p}^{s_p}(\boldsymbol{p})\,\boldsymbol{q}_{\Lambda_q}^{s_q}(\boldsymbol{q}) \left[\frac{\omega_\Lambda^s}{\{1+(\xi_\Lambda^{-s})^2\}\boldsymbol{q}_\Lambda^s(\boldsymbol{k})} - \frac{\omega_{\Lambda_p}^{s_p}}{\{1+(\xi_{\Lambda_p}^{-s_p})^2\}\boldsymbol{q}_{\Lambda_p}^{s_p}(\boldsymbol{p})}\right. \\ &\left. - \frac{\omega_{\Lambda_q}^{s_q}}{\{1+(\xi_{\Lambda_q}^{-s_q})^2\}\boldsymbol{q}_{\Lambda_q}^{s_q}(\boldsymbol{q})}\right] \delta(\Omega_{k,pq})\,\delta_{k,pq}\,\mathrm{d}\boldsymbol{p}\,\mathrm{d}\boldsymbol{q}, \end{aligned} \tag{C 10}$$

where

$$\kappa = \eta\left(\frac{1+P_m(\xi_\Lambda^{-s})^2}{1+(\xi_\Lambda^{-s})^2}\right), \tag{C 11}$$

with $P_m=\nu/\eta$ being the magnetic Prandtl number. These weak turbulence equations are valid for any magnetic Prandtl number. In particular, we note the following relevant limits:

(i) $\kappa=\nu=\eta$ when $P_m=1$;
(ii) $\kappa\rightarrow\nu$ when $kd\rightarrow 0$ and $\Lambda=-s$ (inertial waves);
(iii) $\kappa\rightarrow\eta$ when $kd\rightarrow 0$ and $\Lambda=s$ (magnetostrophic waves);
(iv) $\kappa\rightarrow(\nu+\eta)/2$ when $kd\rightarrow+\infty$ (Alfvén waves).

Appendix D. Exact solutions at constant magnetic helicity flux

In this appendix, we give details of the derivation of the constant magnetic helicity flux solutions (6.16) and (6.17). We start with the weak turbulence equations (6.12):

$$\partial_t H_k = -\frac{\epsilon^2 d}{8b_0}\sum_{s s_p s_q}\int \frac{p_\perp k_\parallel s_p p_\parallel}{q_\perp}\left(\frac{s_q q_\perp - s_p p_\perp}{k_\parallel}\right)^2 (sk_\perp + s_p p_\perp + s_q q_\perp)^2 \sin\theta_q \\ \times\left[\frac{E_q}{q_\perp}(sH_k - s_p H_p) + \frac{s_q H_q}{k_\perp p_\perp}(p_\perp E_k - k_\perp E_p)\right] \\ \times\delta(k_\parallel - p_\parallel - q_\parallel)\,\delta(sk_\perp k_\parallel - s_p p_\perp p_\parallel - s_q q_\perp q_\parallel)\,\mathrm{d}p_\perp\,\mathrm{d}q_\perp\,\mathrm{d}p_\parallel\,\mathrm{d}q_\parallel. \tag{D 1}$$

We define the spectra

$$E(k_\perp, k_\parallel) = C_E k_\perp^n |k_\parallel|^m, \tag{D 2}$$

$$H(k_\perp, k_\parallel) = C_H k_\perp^{\tilde{n}} |k_\parallel|^{\tilde{m}}, \tag{D 3}$$

where C_E and C_H are some constants. We substitute the previous expressions into the weak turbulence equations and obtain, after simple manipulations (e.g. using the identity relation for a triangle),

$$\partial_t H(k_\perp, k_\parallel > 0) = -\frac{\epsilon^2 d}{8b_0}\sum_{s s_p s_q}\int\left(\frac{\sin\theta_k}{k_\perp}\right)p_\perp|k_\parallel|\,|p_\parallel|\left(\frac{s_q q_\perp - s_p p_\perp}{k_\parallel}\right)^2 \\ \times(sk_\perp + s_p p_\perp + s_q q_\perp)^2 C_E C_H\Big[q_\perp^{n-1}|q_\parallel|^m(sk_\perp^{\tilde{n}}|k_\parallel|^{\tilde{m}} - s_p p_\perp^{\tilde{n}}|p_\parallel|^{\tilde{m}}) \\ + s_q q_\perp^{\tilde{n}}|q_\parallel|^{\tilde{m}}(p_\perp^{n-1}|p_\parallel|^m - k_\perp^{n-1}|k_\parallel|^m)\Big]\delta(k_\parallel - p_\parallel - q_\parallel) \\ \times\delta(sk_\perp k_\parallel - s_p p_\perp p_\parallel - s_q q_\perp q_\parallel)\,\mathrm{d}p_\perp\,\mathrm{d}q_\perp\,\mathrm{d}p_\parallel\,\mathrm{d}q_\parallel. \tag{D 4}$$

Then, we split the integral into two identical integrals and apply the Kuznetsov–Zakharov transform on one of them. This yields

$$\partial_t H_k = -\frac{\epsilon^2 d}{16b_0}\sum_{s s_p s_q}\int\left(\frac{\sin\theta_k}{k_\perp}\right)p_\perp|k_\parallel||p_\parallel|\left(\frac{s_q q_\perp - s_p p_\perp}{k_\parallel}\right)^2(sk_\perp + s_p p_\perp + s_q q_\perp)^2 \\ \times C_E C_H\left[q_\perp^{n-1}|q_\parallel|^m(sk_\perp^{\tilde{n}}|k_\parallel|^{\tilde{m}} - s_p p_\perp^{\tilde{n}}|p_\parallel|^{\tilde{m}}) + s_q q_\perp^{\tilde{n}}|q_\parallel|^{\tilde{m}}(p_\perp^{n-1}|p_\parallel|^m - k_\perp^{n-1}|k_\parallel|^m)\right] \\ \times\delta(k_\parallel - p_\parallel - q_\parallel)\,\delta(sk_\perp k_\parallel - s_p p_\perp p_\parallel - s_q q_\perp q_\parallel)\,\mathrm{d}p_\perp\,\mathrm{d}q_\perp\,\mathrm{d}p_\parallel\,\mathrm{d}q_\parallel \\ -\frac{\epsilon^2 d}{16b_0}\sum_{s s_p s_q}\int\left(\frac{\sin\theta_k}{k_\perp}\frac{p_\perp}{k_\perp}\right)\frac{k_\perp^2}{p_\perp}|k_\parallel|\frac{|k_\parallel|^2}{|p_\parallel|}\left[\left(\frac{s_q q_\perp - s_p k_\perp}{p_\parallel}\right)\frac{k_\perp}{p_\perp}\frac{|p_\parallel|}{|k_\parallel|}\right]^2 \\ \times\left((s_p k_\perp + s p_\perp + s_q q_\perp)\frac{k_\perp}{p_\perp}\right)^2 C_E C_H\Big[k_\perp^{n-1}q_\perp^{n-1}p_\perp^{-n+1}|k_\parallel|^m|q_\parallel|^m|p_\parallel|^{-m} \\ \times(sk_\perp^{\tilde{n}}|k_\parallel|^{\tilde{m}} - s_p k_\perp^{2\tilde{n}}p_\perp^{-\tilde{n}}|k_\parallel|^{2\tilde{m}}|p_\parallel|^{-\tilde{m}}) + s_q k_\perp^{\tilde{n}}q_\perp^{\tilde{n}}p_\perp^{-\tilde{n}}|k_\parallel|^{\tilde{m}}|q_\parallel|^{\tilde{m}}|p_\parallel|^{-\tilde{m}} \\ \times(k_\perp^{2n-2}p_\perp^{-n+1}|k_\parallel|^{2m}|p_\parallel|^{-m} - k_\perp^{n-1}|k_\parallel|^m)\Big]\,\delta(k_\parallel + q_\parallel - p_\parallel)\frac{|p_\parallel|}{|k_\parallel|} \\ \times\delta(s_p k_\perp k_\parallel + s_q q_\perp q_\parallel - s p_\perp p_\parallel)\frac{p_\perp|p_\parallel|}{k_\perp|k_\parallel|}\left(\frac{k_\perp|k_\parallel|}{p_\perp|p_\parallel|}\right)^3\,\mathrm{d}p_\perp\,\mathrm{d}q_\perp\,\mathrm{d}p_\parallel\,\mathrm{d}q_\parallel. \tag{D 5}$$

https://doi.org/10.1017/jfm.2014.490 Published online by Cambridge University Press

In the second integral, we interchange the dummy variables s and s_p and use relation (3.26) in the anisotropic limit ($k_\perp \gg k_\parallel$); we obtain

$$
\begin{aligned}
\partial_t H_k = & -\frac{\epsilon^2 d}{16 b_0} \sum_{s s_p s_q} \int \left(\frac{\sin\theta_k}{k_\perp}\right) p_\perp |k_\parallel||p_\parallel| \left(\frac{s_q q_\perp - s_p p_\perp}{k_\parallel}\right)^2 (s k_\perp + s_p p_\perp + s_q q_\perp)^2 \\
& \times C_E C_H \left[q_\perp^{n-1} |q_\parallel|^m (s k_\perp^{\tilde{n}} |k_\parallel|^{\tilde{m}} - s_p p_\perp^{\tilde{n}} |p_\parallel|^{\tilde{m}}) + s_q q_\perp^{\tilde{n}} |q_\parallel|^{\tilde{m}} (p_\perp^{n-1} |p_\parallel|^m - k_\perp^{n-1} |k_\parallel|^m) \right] \\
& \times \delta(k_\parallel - p_\parallel - q_\parallel)\, \delta(s k_\perp k_\parallel - s_p p_\perp p_\parallel - s_q q_\perp q_\parallel)\, \mathrm{d}p_\perp\, \mathrm{d}q_\perp\, \mathrm{d}p_\parallel\, \mathrm{d}q_\parallel \\
& - \frac{\epsilon^2 d}{16 b_0} \sum_{s s_p s_q} \int \left(\frac{\sin\theta_k}{k_\perp}\right) p_\perp |k_\parallel||p_\parallel| \left(\frac{s_q q_\perp - s_p p_\perp}{k_\parallel}\right)^2 (s k_\perp + s_p p_\perp + s_q q_\perp)^2 \left(\frac{k_\perp}{p_\perp}\right)^5 \\
& \times C_E C_H \Big[k_\perp^{n-1} q_\perp^{n-1} p_\perp^{-n+1} |k_\parallel|^m |q_\parallel|^m |p_\parallel|^{-m} (s_p k_\perp^{\tilde{n}} |k_\parallel|^{\tilde{m}} - s k_\perp^{2\tilde{n}} p_\perp^{-\tilde{n}} |k_\parallel|^{2\tilde{m}} |p_\parallel|^{-\tilde{m}}) \\
& + s_q k_\perp^{\tilde{n}} q_\perp^{\tilde{n}} p_\perp^{-\tilde{n}} |k_\parallel|^{\tilde{m}} |q_\parallel|^{\tilde{m}} |p_\parallel|^{-\tilde{m}} (k_\perp^{2n-2} p_\perp^{-n+1} |k_\parallel|^{2m} |p_\parallel|^{-m} - k_\perp^{n-1} |k_\parallel|^m) \Big] \\
& \times \delta(k_\parallel + q_\parallel - p_\parallel)\, \delta(s k_\perp k_\parallel + s_q q_\perp q_\parallel - s_p p_\perp p_\parallel) \\
& \times \left(\frac{k_\perp}{p_\perp}\right)^2 \frac{|k_\parallel|}{|p_\parallel|}\, \mathrm{d}p_\perp\, \mathrm{d}q_\perp\, \mathrm{d}p_\parallel\, \mathrm{d}q_\parallel .
\end{aligned} \tag{D 6}
$$

After some other manipulations, we eventually find that

$$
\begin{aligned}
\partial_t H_k = & -\frac{\epsilon^2 d}{16 b_0} \sum_{s s_p s_q} \int \left(\frac{\sin\theta_k}{k_\perp}\right) p_\perp |p_\parallel| \left(\frac{s_q q_\perp - s_p p_\perp}{k_\parallel}\right)^2 (s k_\perp + s_p p_\perp + s_q q_\perp)^2 \\
& \times \left[\left(\frac{q_\perp}{k_\perp}\right)^{n-1} \left|\frac{q_\parallel}{k_\parallel}\right|^m \left(s - s_p \left(\frac{p_\perp}{k_\perp}\right)^{\tilde{n}} \left|\frac{p_\parallel}{k_\parallel}\right|^{\tilde{m}} \right) \right. \\
& \left. - s_q \left(\frac{q_\perp}{k_\perp}\right)^{\tilde{n}} \left|\frac{q_\parallel}{k_\parallel}\right|^{\tilde{m}} \left(1 - \left(\frac{p_\perp}{k_\perp}\right)^{n-1} \left|\frac{p_\parallel}{k_\parallel}\right|^m \right) \right] C_E C_H k_\perp^{n+\tilde{n}-1} |k_\parallel|^{m+\tilde{m}+1} \\
& \times \left(1 - \left(\frac{p_\perp}{k_\perp}\right)^{-n-\tilde{n}-6} \left|\frac{p_\parallel}{k_\parallel}\right|^{-m-\tilde{m}-1} \right) \delta(k_\parallel - p_\parallel - q_\parallel) \\
& \times \delta(s k_\perp k_\parallel - s_p p_\perp p_\parallel - s_q q_\perp q_\parallel)\, \mathrm{d}p_\perp\, \mathrm{d}q_\perp\, \mathrm{d}p_\parallel\, \mathrm{d}q_\parallel .
\end{aligned} \tag{D 7}
$$

The exact power-law solutions can now be extracted by cancelling the integrand, which corresponds to stationary solutions at constant magnetic helicity flux. The most general solutions (often called the Kolmogorov–Zakharov spectra) are obtained by taking

$$n + \tilde{n} = -6, \tag{D 8}$$

$$m + \tilde{m} = -1. \tag{D 9}$$

Appendix E. Existence of an inverse cascade

In this appendix, we demonstrate the existence of an inverse cascade of magnetic helicity by finding the sign of the magnetic helicity flux. We start with the weak turbulence equation (D 7) characterizing the magnetostrophic regime:

$$\begin{aligned}\partial_t H_k &= -\frac{\epsilon^2 d}{16 b_0} \sum_{s s_p s_q} \int \left(\frac{\sin\theta_k}{k_\perp}\right) p_\perp |p_\parallel| \left(\frac{s_q q_\perp - s_p p_\perp}{k_\parallel}\right)^2 (s k_\perp + s_p p_\perp + s_q q_\perp)^2 \\ &\times \left[\left(\frac{q_\perp}{k_\perp}\right)^{n-1} \left|\frac{q_\parallel}{k_\parallel}\right|^m \left(s - s_p \left(\frac{p_\perp}{k_\perp}\right)^{\tilde{n}} \left|\frac{p_\parallel}{k_\parallel}\right|^{\tilde{m}}\right)\right. \\ &\left. - s_q \left(\frac{q_\perp}{k_\perp}\right)^{\tilde{n}} \left|\frac{q_\parallel}{k_\parallel}\right|^{\tilde{m}} \left(1 - \left(\frac{p_\perp}{k_\perp}\right)^{n-1} \left|\frac{p_\parallel}{k_\parallel}\right|^m\right)\right] C_E C_H k_\perp^{n+\tilde{n}-1} |k_\parallel|^{m+\tilde{m}+1} \\ &\times \left(1 - \left(\frac{p_\perp}{k_\perp}\right)^{-n-\tilde{n}-6} \left|\frac{p_\parallel}{k_\parallel}\right|^{-m-\tilde{m}-1}\right) \delta(k_\parallel - p_\parallel - q_\parallel) \\ &\times \delta(k_\perp |k_\parallel| - p_\perp |p_\parallel| - q_\perp |q_\parallel|)\, \mathrm{d}p_\perp\, \mathrm{d}q_\perp\, \mathrm{d}p_\parallel\, \mathrm{d}q_\parallel. \end{aligned} \tag{E 1}$$

Additionally, we have (Zakharov *et al.* 1992)

$$\partial_t H_k = -\nabla \cdot \boldsymbol{P} = -\frac{1}{k_\perp} \frac{\partial (k_\perp P_\perp)}{\partial k_\perp} - \frac{\partial P_\parallel}{\partial k_\parallel}, \tag{E 2}$$

where $\boldsymbol{P}$ is the magnetic helicity flux vector, with $P_\perp$ and $P_\parallel$ being the perpendicular and parallel components of this flux vector, respectively (axisymmetric turbulence is assumed). Upon introducing the notation $\tilde{p}_\perp \equiv p_\perp/k_\perp$, $\tilde{q}_\perp \equiv q_\perp/k_\perp$, $\tilde{p}_\parallel \equiv |p_\parallel|/|k_\parallel|$ and $\tilde{q}_\parallel \equiv |q_\parallel|/|k_\parallel|$, we obtain

$$\partial_t H_k = \epsilon^2 \frac{d}{b_0} C_E C_H k_\perp^{n+\tilde{n}+4} |k_\parallel|^{m+\tilde{m}}\, I(m, n, \tilde{m}, \tilde{n}) \tag{E 3}$$

with

$$\begin{aligned} I(m, n, \tilde{m}, \tilde{n}) &= -\frac{1}{16} \sum_{s s_p s_q} \int \sqrt{1 - \left(\frac{\tilde{p}_\perp^2 + \tilde{q}_\perp^2 - 1}{2 \tilde{p}_\perp \tilde{q}_\perp}\right)^2}\, \tilde{p}_\perp \tilde{p}_\parallel \left(s_q \tilde{q}_\perp - s_p \tilde{p}_\perp\right)^2 \\ &\times (s + s_p \tilde{p}_\perp + s_q \tilde{q}_\perp)^2 \left[\tilde{q}_\perp^{n-1} \tilde{q}_\parallel^m \left(s - s_p \tilde{p}_\perp^{\tilde{n}} \tilde{p}_\parallel^{\tilde{m}}\right)\right. \\ &\left. - s_q \tilde{q}_\perp^{\tilde{n}} q_\parallel^{\tilde{m}} \left(1 - \tilde{p}_\perp^{n-1} \tilde{p}_\parallel^m\right)\right] \left(1 - \tilde{p}_\perp^{-n-\tilde{n}-6} \tilde{p}_\parallel^{-m-\tilde{m}-1}\right) \\ &\times \delta(s - s_p \tilde{p}_\parallel - s_q \tilde{q}_\parallel)\, \delta(1 - \tilde{p}_\perp \tilde{p}_\parallel - \tilde{q}_\perp \tilde{q}_\parallel)\, \mathrm{d}\tilde{p}_\perp\, \mathrm{d}\tilde{q}_\perp\, \mathrm{d}\tilde{p}_\parallel\, \mathrm{d}\tilde{q}_\parallel. \end{aligned} \tag{E 4}$$

From the flux equation (E 2), we obtain that at constant $k_\parallel$,

$$\frac{\partial (k_\perp P_\perp)}{\partial k_\perp} = -\epsilon^2 \frac{d}{b_0} C_E C_H k_\perp^{n+\tilde{n}+5} |k_\parallel|^{m+\tilde{m}}\, I(m, n, \tilde{m}, \tilde{n}). \tag{E 5}$$

After an integration, we have the general relation

$$P_\perp = -\epsilon^2 \frac{d}{b_0} C_E C_H k_\perp^{n+\tilde{n}+5} |k_\parallel|^{m+\tilde{m}} \frac{I(m, n, \tilde{m}, \tilde{n})}{n + \tilde{n} + 6}. \tag{E 6}$$

The constant flux solution (D 8) that we seek corresponds precisely to the cancellation of the denominator and the numerator I. This indeterminacy can be evaluated using L'Hospital's rule; for this solution we find that

$$P_\perp = \epsilon^2 \frac{d}{b_0} \frac{C_E C_H}{k_\perp |k_\parallel|} A, \tag{E 7}$$

with (upon introducing the exact solutions (D 8) and (D 9))

$$A = \left(\frac{\partial I(m, n, \tilde{m}, \tilde{n})}{\partial (n + \tilde{n} + 6)} \right)_{n+\tilde{n}=-6,\, m+\tilde{m}=-1} \tag{E 8}$$

$$\begin{aligned} &= \frac{1}{16} \sum_{s s_p s_q} \int \sqrt{1 - \left(\frac{\tilde{p}_\perp^2 + \tilde{q}_\perp^2 - 1}{2\tilde{p}_\perp \tilde{q}_\perp} \right)^2}\, \tilde{p}_\perp \tilde{p}_\parallel \left(s_q \tilde{q}_\perp - s_p \tilde{p}_\perp \right)^2 \\ &\quad \times (s + s_p \tilde{p}_\perp + s_q \tilde{q}_\perp)^2 \ln(\tilde{p}_\perp) \left[\tilde{q}_\perp^{n-1} \tilde{q}_\parallel^m \left(s - s_p \tilde{p}_\perp^{-n-6} \tilde{p}_\parallel^{-m-1} \right) \right. \\ &\quad \left. - s_q \tilde{q}_\perp^{-n-6} q_\parallel^{-m-1} \left(1 - \tilde{p}_\perp^{n-1} \tilde{p}_\parallel^m \right) \right] \delta(s - s_p \tilde{p}_\parallel - s_q \tilde{q}_\parallel) \\ &\quad \times \delta(1 - \tilde{p}_\perp \tilde{p}_\parallel - \tilde{q}_\perp \tilde{q}_\parallel)\, \mathrm{d}\tilde{p}_\perp\, \mathrm{d}\tilde{q}_\perp\, \mathrm{d}\tilde{p}_\parallel\, \mathrm{d}\tilde{q}_\parallel. \end{aligned} \tag{E 9}$$

The sign of A can be investigated numerically (the constants C_E and C_H are taken to be positive): a negative sign is found for different values of (n, m) (satisfying the conditions (6.18) and (6.19)), which proves the presence of an inverse cascade in the transverse direction.

In a similar way, from the flux equation (E 2) we find that at constant $k_\perp$,

$$\frac{\partial P_\parallel}{\partial k_\parallel} = -\epsilon^2 \frac{d}{b_0} C_E C_H k_\perp^{n+\tilde{n}+4} |k_\parallel|^{m+\tilde{m}} I(m, n, \tilde{m}, \tilde{n}). \tag{E 10}$$

After an integration, we find the general relation

$$P_\parallel = -\epsilon^2 \frac{d}{b_0} C_E C_H k_\perp^{n+\tilde{n}+4} |k_\parallel|^{m+\tilde{m}+1} \frac{I(m, n, \tilde{m}, \tilde{n})}{m + \tilde{m} + 1}. \tag{E 11}$$

As above, the constant flux solution (D 9) corresponds to cancellation of the denominator and I. Thanks to L'Hospital's rule, we find that

$$P_\parallel = \epsilon^2 \frac{d}{b_0} \frac{C_E C_H}{k_\perp^2} B, \tag{E 12}$$

with (upon introducing the solutions (D 8) and (D 9))

$$B = \left(\frac{\partial I(m, n, \tilde{m}, \tilde{n})}{\partial (m + \tilde{m} + 1)} \right)_{n+\tilde{n}=-6,\, m+\tilde{m}=-1} \tag{E 13}$$

$$\begin{aligned} &= \frac{1}{16} \sum_{s s_p s_q} \int \sqrt{1 - \left(\frac{\tilde{p}_\perp^2 + \tilde{q}_\perp^2 - 1}{2\tilde{p}_\perp \tilde{q}_\perp} \right)^2}\, \tilde{p}_\perp \tilde{p}_\parallel \left(s_q \tilde{q}_\perp - s_p \tilde{p}_\perp \right)^2 \\ &\quad \times (s + s_p \tilde{p}_\perp + s_q \tilde{q}_\perp)^2 \ln(\tilde{p}_\parallel) \left[\tilde{q}_\perp^{n-1} \tilde{q}_\parallel^m \left(s - s_p \tilde{p}_\perp^{-n-6} \tilde{p}_\parallel^{-m-1} \right) \right. \end{aligned}$$

$$- s_q \tilde{q}_\perp^{-n-6} q_\parallel^{-m-1} \left(1 - \tilde{p}_\perp^{n-1} \tilde{p}_\parallel^{m}\right)\Big] \delta(s - s_p \tilde{p}_\parallel - s_q \tilde{q}_\parallel)$$
$$\times \delta(1 - \tilde{p}_\perp \tilde{p}_\parallel - \tilde{q}_\perp \tilde{q}_\parallel)\, \mathrm{d}\tilde{p}_\perp\, \mathrm{d}\tilde{q}_\perp\, \mathrm{d}\tilde{p}_\parallel\, \mathrm{d}\tilde{q}_\parallel. \tag{E 14}$$

The sign of B has also been evaluated numerically for different values of (n, m) (satisfying the conditions (6.18) and (6.19)). A negative sign is found, which demonstrates that the parallel cascade is inverse. This cascade is, however, expected to be much weaker than the perpendicular one, since the combination of relations (E 7) and (E 12) gives in particular the flux ratio (we recall that $k_\parallel \ll k_\perp$)

$$\frac{P_\parallel}{P_\perp} = \frac{k_\parallel}{k_\perp} \frac{B}{A}, \tag{E 15}$$

which is small because A and B are of the same order (as verified numerically).

REFERENCES

BARDINA, J., FERZIGER, J. H. & ROGALLO, R. S. 1985 Effect of rotation on isotropic turbulence: computation and modelling. *J. Fluid Mech.* **154**, 321–336.

BAROUD, C. N., PLAPP, B. B., SHE, Z.-S. & SWINNEY, H. L. 2002 Anomalous self-similarity in a turbulent rapidly rotating fluid. *Phys. Rev. Lett.* **88** (11), 114501.

BARTELLO, P., METAIS, O. & LESIEUR, M. 1994 Coherent structures in rotating three-dimensional turbulence. *J. Fluid Mech.* **273**, 1–29.

BELLET, F., GODEFERD, F. S., SCOTT, J. F. & CAMBON, C. 2006 Wave turbulence in rapidly rotating flows. *J. Fluid Mech.* **562**, 83–121.

BENNEY, D. J. & NEWELL, A. C. 1967 Sequential time closures for interacting random waves. *J. Math. Phys.* **46**, 363–393.

BENNEY, D. J. & NEWELL, A. C. 1969 Random wave closures. *Stud. Appl. Maths* **48**, 29–53.

BENNEY, D. J. & SAFFMAN, P. G. 1966 Nonlinear interactions of random waves in a dispersive medium. *Proc. R. Soc. Lond.* A **289**, 301–320.

BERHANU, M., MONCHAUX, R., FAUVE, S., MORDANT, N., PÉTRÉLIS, F., CHIFFAUDEL, A., DAVIAUD, F., DUBRULLE, B., MARIÉ, L., RAVELET, F., BOURGOIN, M., ODIER, P., PINTON, J.-F. & VOLK, R. 2007 Magnetic field reversals in an experimental turbulent dynamo. *Europhys. Lett.* **77**, 59001.

BIGOT, B. & GALTIER, S. 2011 Two-dimensional state in driven magnetohydrodynamic turbulence. *Phys. Rev.* E **83** (2), 026405.

BIGOT, B., GALTIER, S. & POLITANO, H. 2008 Development of anisotropy in incompressible magnetohydrodynamic turbulence. *Phys. Rev.* E **78** (6), 066301.

BOUROUIBA, L. 2008 Discreteness and resolution effects in rapidly rotating turbulence. *Phys. Rev.* E **78** (5), 056309.

BRAGINSKY, S. I. & ROBERTS, P. H. 1995 Equations governing convection in Earth's core and the geodynamo. *Geophys. Astrophys. Fluid Dyn.* **79**, 1–97.

BRANDENBURG, A. 2001 The inverse cascade and nonlinear alpha-effect in simulations of isotropic helical hydromagnetic turbulence. *Astrophys. J.* **550**, 824–840.

CAMBON, C. & JACQUIN, L. 1989 Spectral approach to non-isotropic turbulence subjected to rotation. *J. Fluid Mech.* **202**, 295–317.

CAMBON, C., MANSOUR, N. N. & GODEFERD, F. S. 1997 Energy transfer in rotating turbulence. *J. Fluid Mech.* **337**, 303–332.

CHEN, Q., CHEN, S. & EYINK, G. L. 2003*a* The joint cascade of energy and helicity in three-dimensional turbulence. *Phys. Fluids* **15**, 361–374.

CHEN, Q., CHEN, S., EYINK, G. L. & HOLM, D. D. 2003*b* Intermittency in the joint cascade of energy and helicity. *Phys. Rev. Lett.* **90** (21), 214503.

CHO, J. 2011 Magnetic helicity conservation and inverse energy cascade in electron magnetohydrodynamic wavepackets. *Phys. Rev. Lett.* **106** (19), 191104.

CRAYA, A. 1954 *Contribution à l'analyse de la turbulence associée à des vitesses moyennes. (Publications Scientifiques et Techniques du Ministère de l'Air, vol. 345)*, Ministère de l'Air, France.

DAVIDSON, P. A. 2004 *Turbulence: An Introduction for Scientists and Engineers*. Oxford University Press.

DORMY, E., VALET, J.-P. & COURTILLOT, V. 2000 Numerical models of the geodynamo and observational constraints. *Geochem. Geophys. Geosyst.* **1**, 1037–1042.

DYACHENKO, S., NEWELL, A. C., PUSHKAREV, A. & ZAKHAROV, V. E. 1992 Optical turbulence: weak turbulence, condensates and collapsing filaments in the nonlinear Schrödinger equation. *Physica* D **57**, 96–160.

FALCON, É., LAROCHE, C. & FAUVE, S. 2007 Observation of gravity–capillary wave turbulence. *Phys. Rev. Lett.* **98** (9), 094503.

FAVIER, B. F. N., GODEFERD, F. S. & CAMBON, C. 2012 On the effect of rotation on magnetohydrodynamic turbulence at high magnetic Reynolds number. *Geophys. Astrophys. Fluid Dyn.* **106**, 89–111.

FINLAY, C. C. 2008 Waves in the presence of magnetic fields, rotation and convection. In *Dynamos, Session 88: Lecture Notes of the Les Houches Summer School 2007* (ed. P. Cardin & L. F. Cugliandolo), pp. 403–450. Elsevier.

FINLAY, C. C., DUMBERRY, M., CHULLIAT, A. & PAIS, M. A. 2010 Short timescale core dynamics: theory and observations. *Space Sci. Rev.* **155**, 177–218.

FINLAY, C. C. & JACKSON, A. 2003 Equatorially dominated magnetic field change at the surface of Earth's core. *Science* **300**, 2084–2086.

FRISCH, U. 1995 *Turbulence: the Legacy of A. N. Kolmogorov*. Cambridge University Press.

GALTIER, S. 2003 Weak inertial-wave turbulence theory. *Phys. Rev.* E **68** (1), 015301.

GALTIER, S. 2006*a* Multi-scale turbulence in the inner solar wind. *J. Low Temp. Phys.* **145**, 59–74.

GALTIER, S. 2006*b* Wave turbulence in incompressible Hall magnetohydrodynamics. *J. Plasma Phys.* **72**, 721–769.

GALTIER, S. 2009*a* Exact vectorial law for homogeneous rotating turbulence. *Phys. Rev.* E **80**, 046301.

GALTIER, S. 2009*b* Wave turbulence in magnetized plasmas. *Nonlinear Process. Geophys.* **16**, 83–98.

GALTIER, S. 2014 Theory for helical turbulence under fast rotation. *Phys. Rev.* E **89**, 041001(R).

GALTIER, S. & BHATTACHARJEE, A. 2003 Anisotropic weak whistler wave turbulence in electron magnetohydrodynamics. *Phys. Plasmas* **10**, 3065–3076.

GALTIER, S. & CHANDRAN, B. D. G. 2006 Extended spectral scaling laws for shear-Alfvén wave turbulence. *Phys. Plasmas* **13** (11), 114505.

GALTIER, S. & NAZARENKO, S. V. 2008 Large-scale magnetic field sustainment by forced MHD wave turbulence. *J. Turbul.* **9**, 40.

GALTIER, S., NAZARENKO, S. V., NEWELL, A. C. & POUQUET, A. 2000 A weak turbulence theory for incompressible magnetohydrodynamics. *J. Plasma Phys.* **63**, 447–488.

GALTIER, S., NAZARENKO, S. V., NEWELL, A. C. & POUQUET, A. 2002 Anisotropic turbulence of shear-Alfvén waves. *Astrophys. J. Lett.* **564**, L49–L52.

GLATZMAIER, G. A. & ROBERTS, P. H. 1995 A three-dimensional self-consistent computer simulation of a geomagnetic field reversal. *Nature* **377**, 203–209.

GREENSPAN, H. P. 1968 *The Theory of Rotating Fluids*. Cambridge University Press.

HASSELMANN, K. 1962 On the nonlinear energy transfer in a gravity-wave spectrum. Part 1. General theory. *J. Fluid Mech.* **12**, 481–500.

HOPFINGER, E. J., GAGNE, Y. & BROWAND, F. K. 1982 Turbulence and waves in a rotating tank. *J. Fluid Mech.* **125**, 505–534.

IROSHNIKOV, P. S. 1964 Turbulence of a conducting fluid in a strong magnetic field. *Sov. Astron.* **7**, 566–571.

JACQUIN, L., LEUCHTER, O., CAMBON, C. & MATHIEU, J. 1990 Homogeneous turbulence in the presence of rotation. *J. Fluid Mech.* **220**, 1–52.

JONES, C. A. 2011 Planetary magnetic fields and fluid dynamos. *Annu. Rev. Fluid Mech.* **43**, 583–614.

KINGSEP, A. S., CHUKBAR, K. V. & YANKOV, V. V. 1990 Electron magnetohydrodynamics. In *Reviews of Plasma Physics, Volume 16* (ed. B. B. Kadomtsev), pp. 243–291. Consultants Bureau.

KOLMAKOV, G. V., LEVCHENKO, A. A., BRAZHNIKOV, M. Y., MEZHOV-DEGLIN, L. P., SILCHENKO, A. N. & MCCLINTOCK, P. V. 2004 Quasiadiabatic decay of capillary turbulence on the charged surface of liquid hydrogen. *Phys. Rev. Lett.* **93** (7), 074501.

KRAICHNAN, R. H. 1965 Inertial range spectrum in hydromagnetic turbulence. *Phys. Fluids* **8**, 1385–1387.

KRAICHNAN, R. H. 1973 Helical turbulence and absolute equilibrium. *J. Fluid Mech.* **59**, 745–752.

KUZNETSOV, E. A. 1972 Turbulence of ion sound in a plasma located in a magnetic field. *Sov. Phys. JETP* **35**, 310–314.

LAMRIBEN, C., CORTET, P.-P. & MOISY, F. 2011 Direct measurements of anisotropic energy transfers in a rotating turbulence experiment. *Phys. Rev. Lett.* **107** (2), 024503.

LEHNERT, B. 1954 Magnetohydrodynamic waves under the action of the coriolis force. *Astrophys. J.* **119**, 647.

LESIEUR, M. 1997 *Turbulence in Fluids*, 3rd edn. Kluwer.

LVOV, Y., NAZARENKO, S. & WEST, R. 2003 Wave turbulence in Bose–Einstein condensates. *Physica* D **184**, 333–351.

MATTHAEUS, W. H. & GOLDSTEIN, M. L. 1982 Measurement of the rugged invariants of magnetohydrodynamic turbulence in the solar wind. *J. Geophys. Res.* **87**, 6011–6028.

MEYRAND, R. & GALTIER, S. 2012 Spontaneous chiral symmetry breaking of Hall MHD turbulence. *Phys. Rev. Lett.* **109**, 194501.

MININNI, P. D. & POUQUET, A. 2009 Helicity cascades in rotating turbulence. *Phys. Rev.* E **79** (2), 026304.

MININNI, P. D. & POUQUET, A. 2010*a* Rotating helical turbulence. I. Global evolution and spectral behavior. *Phys. Fluids* **22** (3), 035105.

MININNI, P. D. & POUQUET, A. 2010*b* Rotating helical turbulence. II. Intermittency, scale invariance, and structures. *Phys. Fluids* **22** (3), 035106.

MININNI, P. D., ROSENBERG, D. & POUQUET, A. 2012 Isotropization at small scales of rotating helically driven turbulence. *J. Fluid Mech.* **699**, 263–279.

MOFFATT, H. K. 1969 The degree of knottedness of tangled vortex lines. *J. Fluid Mech.* **35**, 117–129.

MOFFATT, H. K. 1970 Dynamo action associated with random inertial waves in a rotating conducting fluid. *J. Fluid Mech.* **44**, 705–719.

MOFFATT, H. K. 1972 An approach to a dynamic theory of dynamo action in a rotating conducting fluid. *J. Fluid Mech.* **53**, 385–399.

MOFFATT, H. K. 1978 *Magnetic Field Generation in Electrically Conducting Fluids*. Cambridge University Press.

MORIN, J., DORMY, E., SCHRINNER, M. & DONATI, J.-F. 2011 Weak- and strong-field dynamos: from the Earth to the stars. *Mon. Not. R. Astron. Soc.* **418**, L133–L137.

MORIZE, C., MOISY, F. & RABAUD, M. 2005 Decaying grid-generated turbulence in a rotating tank. *Phys. Fluids* **17** (9), 095105.

NAZARENKO, S. 2011 *Wave Turbulence*, Lecture Notes in Physics, vol. 825. Springer.

NEWELL, A. C., NAZARENKO, S. & BIVEN, L. 2001 Wave turbulence and intermittency. *Physica* D **152**, 520–550.

PARKER, E. N. 1958 Dynamics of the interplanetary gas and magnetic fields. *Astrophys. J.* **128**, 664–676.

PEREZ, J. C. & BOLDYREV, S. 2008 On weak and strong magnetohydrodynamic turbulence. *Astrophys. J. Lett.* **672**, L61–L64.

PÉTRÉLIS, F., MORDANT, N. & FAUVE, S. 2007 On the magnetic fields generated by experimental dynamos. *Geophys. Astrophys. Fluid Dyn.* **101**, 289–323.

POUQUET, A., FRISCH, U. & LEORAT, J. 1976 Strong MHD helical turbulence and the nonlinear dynamo effect. *J. Fluid Mech.* **77**, 321–354.

RIEUTORD, M., TRIANA, S. A., ZIMMERMAN, D. S. & LATHROP, D. P. 2012 Excitation of inertial modes in an experimental spherical Couette flow. *Phys. Rev.* E **86** (2), 026304.

ROBERTS, P. H. & KING, E. M. 2013 On the genesis of the Earth's magnetism. *Rep. Prog. Phys.* **76** (9), 096801.

SAGDEEV, R. Z. & GALEEV, A. A. 1969 *Nonlinear Plasma Theory*, W.A. Benjamin.

SAHRAOUI, F., GALTIER, S. & BELMONT, G. 2007 On waves in incompressible Hall magnetohydrodynamics. *J. Plasma Phys.* **73**, 723–730.

SCHMITT, D., ALBOUSSIÈRE, T., BRITO, D., CARDIN, P., GAGNIÈRE, N., JAULT, D. & NATAF, H.-C. 2008 Rotating spherical Couette flow in a dipolar magnetic field: experimental study of magneto-inertial waves. *J. Fluid Mech.* **604**, 175–197.

SCOTT, J. F. 2014 Wave turbulence in a rotating channel. *J. Fluid Mech.* **741**, 316–349.

SHAIKH, D. & ZANK, G. P. 2005 Driven dissipative whistler wave turbulence. *Phys. Plasmas* **12** (12), 122310.

SHEBALIN, J. V. 2006 Ideal homogeneous magnetohydrodynamic turbulence in the presence of rotation and a mean magnetic field. *J. Plasma Phys.* **72**, 507–524.

SHIRLEY, J. H. & FAIRBRIDGE, R. W. 1997 *Encyclopedia of Planetary Sciences*. Springer.

SMITH, L. M. & LEE, Y. 2005 On near resonances and symmetry breaking in forced rotating flows at moderate Rossby number. *J. Fluid Mech.* **535**, 111–142.

SMITH, L. M. & WALEFFE, F. 1999 Transfer of energy to two-dimensional large scales in forced, rotating three-dimensional turbulence. *Phys. Fluids* **11**, 1608–1622.

STANLEY, S. & BLOXHAM, J. 2006 Numerical dynamo models of Uranus' and Neptune's magnetic fields. *Icarus* **184**, 556–572.

STEVENSON, D. J. 2003 Planetary magnetic fields. *Earth Planet. Sci. Lett.* **208**, 1–11.

TASSOUL, J.-L. 2000 *Stellar Rotation*. Cambridge University Press.

TEITELBAUM, T. & MININNI, P. D. 2009 Effect of helicity and rotation on the free decay of turbulent flows. *Phys. Rev. Lett.* **103** (1), 014501.

TURNER, L. 2000 Using helicity to characterize homogeneous and inhomogeneous turbulent dynamics. *J. Fluid Mech.* **408**, 205–238.

VAN BOKHOVEN, L. J. A., CLERCX, H. J. H., VAN HEIJST, G. J. F. & TRIELING, R. R. 2009 Experiments on rapidly rotating turbulent flows. *Phys. Fluids* **21** (9), 096601.

WALEFFE, F. 1992 The nature of triad interactions in homogeneous turbulence. *Phys. Fluids* **4**, 350–363.

WALEFFE, F. 1993 Inertial transfers in the helical decomposition. *Phys. Fluids* **5**, 677–685.

ZAKHAROV, V. E. 1965 Weak turbulence in media with a decay spectrum. *J. Appl. Mech. Tech. Phys.* **6**, 22–24.

ZAKHAROV, V. E. 1967 On the spectrum of turbulence in plasma without magnetic field. *J. Expl Theor. Phys.* **24**, 455–459.

ZAKHAROV, V. E. & FILONENKO, N. N. 1966 The energy spectrum for stochastic oscillations of a fluid surface. *Dokl. Akad. Nauk SSSR* **170**, 1292–1295.

ZAKHAROV, V. E., L'VOV, V. S. & FALKOVICH, G. 1992 *Kolmogorov Spectra of Turbulence I: Wave Turbulence*, Springer Series in Nonlinear Dynamics. Springer.